



CHALMERS
UNIVERSITY OF TECHNOLOGY



Analysis of forces and displacement in floating pile with different analytical methods

A case study of Lilla-Bommen-Marieholm tunnel foundation

Master's Thesis in the Master's Programme Infrastructure and Environmental Engineering

OKORIE CHIDIEBERE ANTHONY

Department of Architecture and Civil Engineering
Division of Geology and Geotechnics
CHALMERS UNIVERSITY OF TECHNOLOGY
Gothenburg, Sweden 2017
Master's Thesis BOMX02-17-76

Analysis of forces and displacement in floating pile with different analytical methods

A case study of Lilla-Bommen-Marieholm tunnel foundation

OKORIE CHIDIEBERE ANTHONY

Analysis of forces and displacement in floating pile with different analytical methods

A case study of Lilla-Bommen-Marieholm tunnel foundation.

OKORIE CHIDIEBERE ANTHONY

© OKORIE CHIDIEBERE ANTHONY 2017

Examiner: Associate Professor Jelke Dijkstra, Department of Architecture and Civil Engineering, Division Geology and Geotechnics

Department of Architecture and Civil Engineering
Division of Geology and Geotechnics
Chalmers University of Technology
SE-412 96 Gothenburg, Sweden
Telephone: + 46 (0)31-772 1000

Cover:

A picture of Reinforcement wall of tunnel at Lilla-Bommen-Marieholm tunnel.

Chalmers Reproservice Gothenburg, Sweden 2017

Analysis of forces and displacement in floating pile with different analytical methods
A case study of Lilla-Bommen-Marieholm tunnel foundation

Master's thesis in the Master's Programme Infrastructure and Environmental Engineering

OKORIE CHIDIEBERE ANTHONY

Department of Architecture and Civil Engineering
Division of Geology and Geotechnics
Chalmers University of Technology

ABSTRACT

In Lilla-Bommen-Marieholm Section of E45 highway, Swedish Transport Administration Agency (Trafikverket), proposed a tunnel to expand infrastructure and easy expected high traffic in near future. The foundation of tunnel, is approximately 250 000 m long floating concrete piles. The piles where designed with Finite Element Method calculation with experiences of short piles. Due to method of design, heavy loads expected and settlement nature of soft clay found in the section, instrumented piles where included to study behaviour of the piles and its capacity.

This report presents, load distribution in a long floating pile as function of pile head load and down drag effect. Also installation effects on instrumented pile investigated. Zhang's Load transfer- softening nonlinear model of skin resistance and bilinear base load-displacement model and neutral plane approach were also used in analysis. Two case studies of instrumented pile in Gothenburg region where examined, literature studies and interview with one of the involved person.

The result of the load – settlement analysis, shows that at the pile head load of 3000kN on a pile length of 65m, nonlinear relationship exist between the skin resistance and displacement. Also, displacements and load distributions were linear, decreasing with depth. Pile head settlement of 0.052m, end displacement of 2×10^{-4} m with base load of 127.8kN observed. With neutral plane approach, the neutral plane was found to be at 32m depth. Total settlement below the neutral plane was 0.638m with average strain of 1.2% and pile capacity is 3582KN. With this approach, pile behaviour was good enough compared with all the theories cut across in the study.

Investigation on the installation effects on pile instrumentation, shows that challenges starts with human error in calculation and improper placement of the instrumentation equipment. Hammer blows from installation process, incorrect prediction of strength of soil layers in relative to hammer impact from the installation and pore water penetration are the causes of failures observed.

Key words: Floating pile, End displacement, E45, Settlement, Softening, Skin resistance, Instrumentation, Pile head load, Strain, Tunnel, Foundation

Svensk översättning av titeln
Underrubrik (Om sådan finns)

Examensarbete inom masterprogrammet Infrastructure and Environmental
Engineering

OKORIE CHIDIEBERE ANTHONY
Avdelning för Arkitektur och civilingenjör

Division av geologi och geoteknik
Chalmers tekniska högskola

SAMMANFATTNING

I samband med nedsänkningen av motorvägen E45, sträckan Lilla-Bommen-Marieholm, har Trafikverket föreslagit att en del av denna ska utgöras av en tunnel. Syftet med projektet är att förbättra infrastrukturen med anledning av den ökade trafiken och stadens framtida möjligheter till vidare exploatering. Grundläggningen av tunneldelen utgörs av ca 250 000 m långa betongpålar. Pålarna är designade med hjälp av numeriska beräkningar och analyserna baseras på erfarenhet av kortare pålar. På grund av höga laster samt undergrundens lösa lera måste sättningsproblematiken i området hanteras. Inom ramen för projektet har fyra pålar instrumenterats för att möjliggöra studier av pålarnas beteende och kapacitet.

Föreliggande rapport presenterar lastfördelningen i en lång kohesionspåle som funktion av last och neddragningseffekten. Zhang's metod för lastöverföring och betraktelser av neutrala planet har använts i analysen. Även installationseffekter på den instrumenterade pålen har studerats. Rapporten redogör också för en litteraturstudie och två andra projekt där instrumenterade pålar har använts i Göteborgsregionen.

Resultatet av sättningsanalysen visar att vid en belastning av 3000 kN, på en påle med längden 65 m, ger ett icke-linjärt förhållande mellan mantelytans friktion och den vertikal sättningen. Sättningar och lastfördelningar är linjära och minskar med djupet. Pålhuvudets vertikala rörelse konstaterades vara 0,052 m. Pålpetsens förskjutning var $2 \cdot 10^{-4}$ m och hade en belastning av 127,8 kN. Det neutrala planet återfanns vid 32 m djup. Total sättning under det neutrala planet var 0,638 m med en genomsnittlig töjning om 1,2 % och lastkapaciteten 3582 kN. Analysförfarandet med det neutrala planet är tillräckligt bra jämfört med de teorier som studerats inom ramen för examensarbetet.

Undersökningen av installationseffekter vid instrumentering av pålar visar att utmaningarna ofta ligger i beräkningsskedet, vid val av analysmetod och att inte ha möjlighet att beakta alla effekter, samt felaktigt placerad utrustning. Troliga orsaker till svårigheter, avseende att erhålla kvalitativ mätdata, är slagen från hammaren vid installationsprocessen, felaktig tolkning av jordlagerföljden vilket påverkar hammarens åverkan på utrustningen, samt intrång av vatten i instrumenteringen.

Nyckelord: Kohesionspåle, Ändförskjutning, E45, Sättning, Deformationsmjuknande, Mantelmotstånd, Instrumentation, Pållast, Töjning, Tunnel, Grundläggning

CONTENTS

ABSTRACT	I
SAMMANFATTNING	III
CONTENTS	V
PREFACE	VII
NOTATIONS	VIII
1 INTRODUCTION	1
1.1 Background	1
1.2 Aim and Objectives	1
1.3 Limitation/Scope	2
2 FOUNDATION	3
2.1 Pile Foundation	3
2.1.1 Displacement/Replacement piles	5
2.2 Pile Selection	5
2.3 Geotechnical Bearing capacity of piled foundations	6
2.4 Instrumented pile	6
2.5 Pile Installation	9
2.5.1 Pile Installation Requirements	10
2.6 Stages in Pile Foundation History	10
2.7 Settlements and Consolidation theory	11
2.7.1 Consolidation settlements	11
2.7.2 Settlement of piled foundations	14
2.8 Negative skin friction and Neutral Plane	14
2.9 Piled foundation Analysis	16
2.10 Single pile load-settlement analysis.	17
2.10.1 A softening nonlinear model of skin resistance	17
2.10.2 A bilinear base load-displacement model	18
3 ANALYSIS ALGORITHMS	20
3.1 Neutral plane approach	20
3.2 Load – Settlement analysis method	20
4 CASE STUDY	24
4.1 E45project: Lilla-Bommen-Marieholm tunnel foundation	24
4.1.1 Topography and surface Conditions	25
4.1.2 Geotechnical Conditions	25
4.1.3 Soil profile	25

4.1.4	Soil Parameters	25
4.2	Instrumented pile	26
4.3	Skanska high-rise building, Lilla-Bommen/ Tolo Tvarled instrumented pile	28
5	RESULTS AND DISCUSSION	30
5.1	Neutral plane Approach	30
5.2	Load transfer method	31
5.2.1	Scenario 1: Behaviour of pile as function varying pile head load	31
5.2.2	Scenario 2: Pile stiffness (modulus of elasticity) effect	32
5.2.3	Scenario 3: Down drag effect	34
6	CONCLUSION AND RECOMMENDATION	35
6.1	Conclusion	35
6.2	Recommendation for further study	35
	REFERENCES	36
	APPENDIX	38

PREFACE

This Master's thesis was conducted at the geotechnical department of Tyren AB Gothenburg with Peab AB's E45 tunnel construction site as case study, between January and June 2017.

I wish to use this opportunity to express my gratitude to the coordinating supervisor at companies, Mrs Svahn, Victoria for providing the plat form for this study and her great assistance in providing me with background material used for the analysis. Also, will like to thank Daniel Hägerstrand, Tyren and Michael Sabatini, Peab AB for their great assistance in exposing me to the practical aspects in the subject area.

My heart filled appreciation goes to Jelke Dijkstra, Chalmers University of Technology. Who not only being examiner but acted as academic supervisor when the work gets tough. Thank you for the academic materials made available at the course of this work, which educated my ignorance at the subject area and impacted the knowledge. For taking time to answer my questions and always being available to assist.

Finally, I say thanks to Mrs Okorie Joy Chioma, my loving wife for her understanding and support within the years of this Master's program.

Gothenburg June, 2017

Okorie, Chidiebere Anthony

NOTATIONS

Roman upper case letters

A_s	Area of the pile section at the pile toe
E	Action effect
M_o	Compression modulus when
M_L	Compression modulus when
N_{cp}	Bearing capacity factor for pile toe
R	Geotechnical bearing capacity
R_d	Geotechnical bearing capacity (design value)
R_{toe}	Resistance at pile toe
T_v	Time factor
U_v	Degree of consolidation
Q	Load
Q_m	Load distributed from pile shaft
Q_s	Load distributed from pile toe
A_p	Pile area
E_p	Pile elastic modulus
G_{sb}	Shear modulus of pile base soil
K	Lateral earth pressure coefficient
K_o	In situ earth pressure coefficient
L	Pile length
L_1	Length of pile segment 1
T, T'	Total skin friction or sum of total skin friction and mobilized base load
T_1	Total skin friction of pile segment 1
T^{ave}	Total skin friction or sum of total skin friction and mobilized base load
w_b	Pile-end displacement
w_{b1}	Pile end displacement of pile segment 1
w_{c1}	Vertical movement at the middle height of pile segment 1
Δw_t	Increased settlement at pile head induced by ΔP
D	Diameter of pile

Roman lower case letters

c	Pile spacing
c_u	Undrained shear strength
c_{uk}	Undrained shear strength (unreduced)
c_v	Coefficient of consolidation
d	Drainage distance
f_m	Shaft resistance
s_c	Consolidation settlements
s_i	Immediate settlements
s_s	Secondary consolidation or creep settlements
s_t	Total settlements
u	Pore pressure
Δu	Excess pore water pressure
w_L	Liquid limit
w_N	Water content

a	Parameter used to simulate a softening nonlinear model of skin resistance
b	Parameter used to simulate a softening nonlinear model of skin resistance
c	Parameter used to simulate a softening nonlinear model of skin resistance
k_1	compressive rigidity of pile-tip soil in the first of load-displacement curve
k_2	compressive rigidity of pile-tip soil in the second of load-displacement curve
k_t	ratio of increased pile head load ΔP_t to increased pile head settlement Δw_t
p_1	average axial load of pile segment 1
p_{b1}	mobilized base load of pile segment 1
p_{bm}	mobilized base load of pile segment m
Δp_t	increased load at pile head
P_{t1}	load at pile head of segment 1
s_{bu}	Pile-end displacement related to ultimate end resistance in the first
s_s	Relative shaft displacement
$s_s(z)$	Pile-soil relative displacement at a given depth z
s_{su}	Pile-soil relative displacement corresponding to limiting unit skin
s_∞	Very large value of pile-soil relative displacement
s_{c1}	Elastic deformation of pile segment 1
s_{c1}^1	Modified compression of pile segment 1

Greek letters

γ	Unit weight
γ_{mAs}	Partial factor for variation of circumference at the pile toe
γ_{mcs}	Partial factor for variation of shear strength at the pile toe
γ_{mNcp}	Partial factor for
γ_{mcm}	Partial factor for variation of shear strength along the pile
γ_{ma}	Partial factor for variation of adhesion factor
$\gamma_{m\Theta}$	Partial factor for variation of circumference
γ_n	Partial factor for safety class
γ_w	Unit weight of water
ϵ	Strain
σ'	Effective stress
σ'_o	In-situ stress
σ'_c	Pre consolidation pressure
σ'_v	Effective vertical stress

Abbreviations

CRS	Constant rate of strain
OCR	Over consolidation

1 Introduction

Anisotropic and variable properties of soil in different area, pose challenge and complex situation for geotechnics engineers. To ascertain and have a common model for foundation-soil relative behaviour when on load and settlement nature become task. Use of deep foundation in transmission of load from super structure to a firm strata in sub soil is a common practice in area of soft soils like Gothenburg region in Sweden. Nature of settlements and pattern of load transfer to the soil layer have be major concern in all large construction projects in soft soil. To achieve serviceability limit state in structure; sound analysis and proper understanding of pile-soil relative behaviour is imperative.

1.1 Background

City developments and technology advancement places high demand on existing buildings and infrastructures. In Lilla-Bommen-Mariaholm section of E45 highway, Swedish Transport Administration Agency (Trafikverket), proposed a tunnel to expand infrastructure and easy expected high-volume traffic in near future.

The foundation of tunnel, is founded on deep layered clay. Approximately 250 000 m long floating concrete piles will be installed in the foundation. The piles where designed with FEM calculation with experiences of short piles. Due to method of design, heavy loads expected and settlement nature of soft clay found in the section. Instrumented piles where included to study behaviour of the piles and its capacity.

Due to uncertainties in the method of design of the foundation and assumptions made, four instrumented piles will be installed to measure forces, movements and pore pressure in the earth. Also, to study the piled foundation capacity and settlement nature of long floating piles in soft clay. Analysis of these made to ascertain the behaviour of the piles in short and long term for future references.

1.2 Aim and Objectives

The purpose of this project is to study the

The aim of this master thesis is to study forces and displacements in long floating pile in soft clay as a function of pile load and background settlement at Lilla-Bommen-Mariaholm tunnel project. Also, effects of installations process on instrumentation.

This aim will be accomplished through the following objectives;

- Use of Zhang's load transfer method to analysis forces and displacements in the pile segments.
- Application of Neutral plane approach to detect a frictionless zone, strains and settlement below the plane.
- Study of past pile instrumented reports and interview with person(s) involved in the project to understand the steps adopted and challenge(s) encountered.
- Desktop study of pile analysis methods, instrumentation & installation procedures.

1.3 Limitation/Scope

The work will focus on analysis of floating pile in soft clay, instrumentation and installation processes of floating piles. The study considers only one-dimensional displacements i.e. vertically, lateral displacements and deformation in pile element are neglected. The analysis of pile where limited to single.

2 Foundation

Foundation is integral part a structure which holds and transmits superstructure and other loads to firm strata of soil at acceptable settlement. They are two basic types: **shallow foundation** -footings/raft or **deep foundation** - piles, piers or caissons foundation. According to Knappett & Craig (2012), shallow foundations width are often greater than their depth, while deep are those which ratio of depth to breath is greater than or equal to one. The type to use depends on load to be transmitted, soil bearing capacity, slope of the soil, geotechnical conditions etc. However, to perform satisfactorily, its designed should meet two principal requirements; **ultimate limit states** and **serviceability limit states** (Knappett & Craig, 2012).

2.1 Pile Foundation

In certain situations, use of shallow foundation is uneconomical and unsafe. When design loads are large, near surface soils have low stiffness, soil layers are inclined, settlement sensitive structured are to be build, in marine environments where tidal, wave or flow actions are anticipated. In such situation(s) deep foundation becomes necessary to have stable and safe substructure (Knappett & Craig, 2012).

Pile is the most common type of deep foundation, which is a column of concrete, steel or timber installed in ground. It may be circular or square in section with outside diameter (D_o) or width (B_p) that is very much smaller than their length (L_p), i.e. $L_p \gg D_o$ (Knappett & Craig, 2012). Common in parts of the world with glacial or alluvial sediments and area with quaternary geology. Its main function is to transfer loads from superstructure to deep layers of soil (Claes, 2012). It is commonly subjected to compression loads (Yanne, 2016).

According to Alen C., 2009 and (Knappett & Craig, 2012), Piles are classified into different types based on;

- material of pile elements - steel, pre-cast concrete, In-situ casted concrete or timber piles;
- installation method and effect of installation - driven/displacement and bored piles;
- type of soil the piles are installed in – Friction/Cohesion/floating Pile and
- Way the piles are loaded -Axially loaded (compression or tension) and transversally loaded piles.

Commonly classified based on pattern of installation as displacement and non-displacement/replacement piles. In summary, it is classified as illustrated in Figure 2.1.

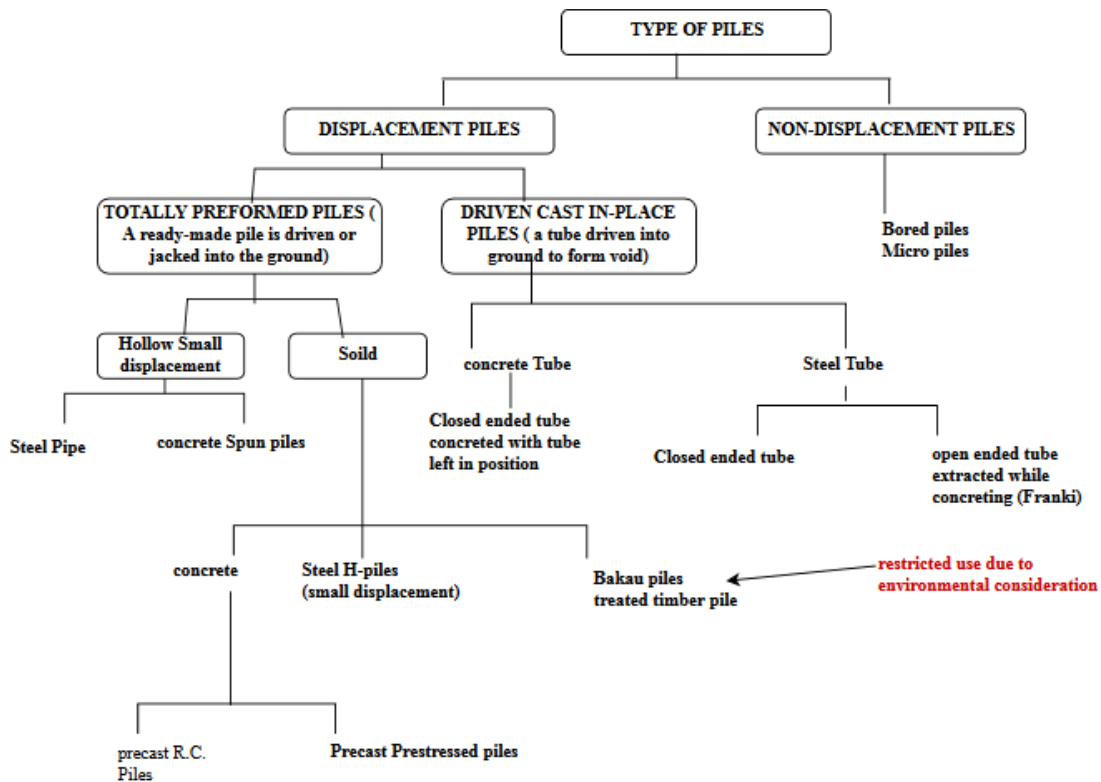


Figure 2.1: Classification of piled foundation (Sew & Meng, 2017).

From the geotechnical aspects, piled foundations are further classified based on load bearing capacity as **shaft bearing piles**, **end bearing piles** and/or **combination of both types**.

Friction piles are piles installed in frictional material, it drives most of its bearing capacity from toe and normally analysed based on effective stress analysis. While cohesion often called, floating piles are piles in clay, its bearing capacity are mainly from its shaft and can be analyse with the total stress concept. Figure 2.3, illustrate pile foundation classification based on load bearing ability.

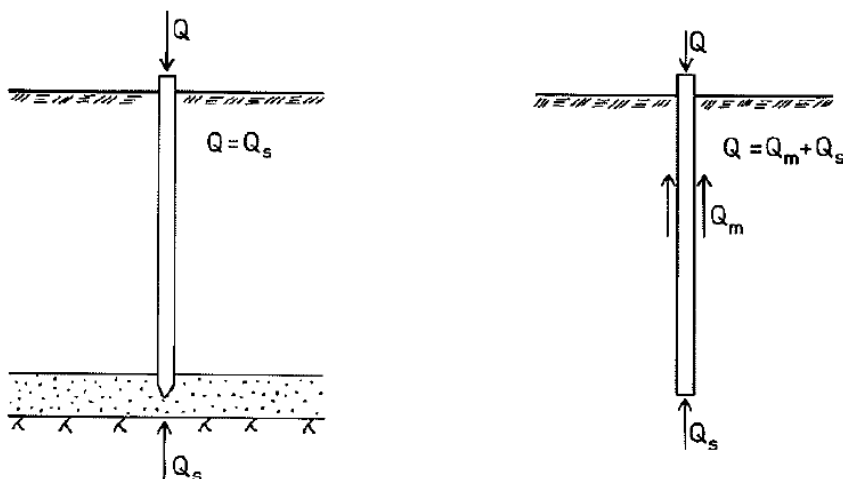


Figure 2.2: Bearing piles (a) End-bearing pile (b) Shaft bearing pile (Claes, 2012)

2.1.1 Displacement/Replacement piles

According Yannie J, 2016, method of pile installation has effect on the pile cycle. In displacement method, pile is driven into the ground with aid of jack or hammer while in replacement method hole is bored and soil remove before pile is driven into bored hole. There is no displacement of soil. In the displacement method soil at the toe is distorted, pushed downward and displaced laterally at the process of installation, causing remoulding of the soil structure and increase in total stresses in the soil. The tension loads are generated at process from the stress wave in the pile, this wave can lead to crack in concrete, hence reducing the cross-section stiffness and exposing steel reinforcement to corrosion (Yanne, 2016).

2.2 Pile Selection

The choice of pile to use are influenced by the following factors:

- Installation method
- Type of piles available in market
- Contractual requirements
- Ground conditions (e.g. Limestone, etc.)
- Site conditions and constraints (e.g. Accessibility)
- Type and magnitude of loading
- Development program (Sew & Meng, 2017) and cost (Sew & Meng, 2017).

The flow chart in Figure 2.3 illustrate pattern of pile selection putting into consideration all the factors mentioned above.

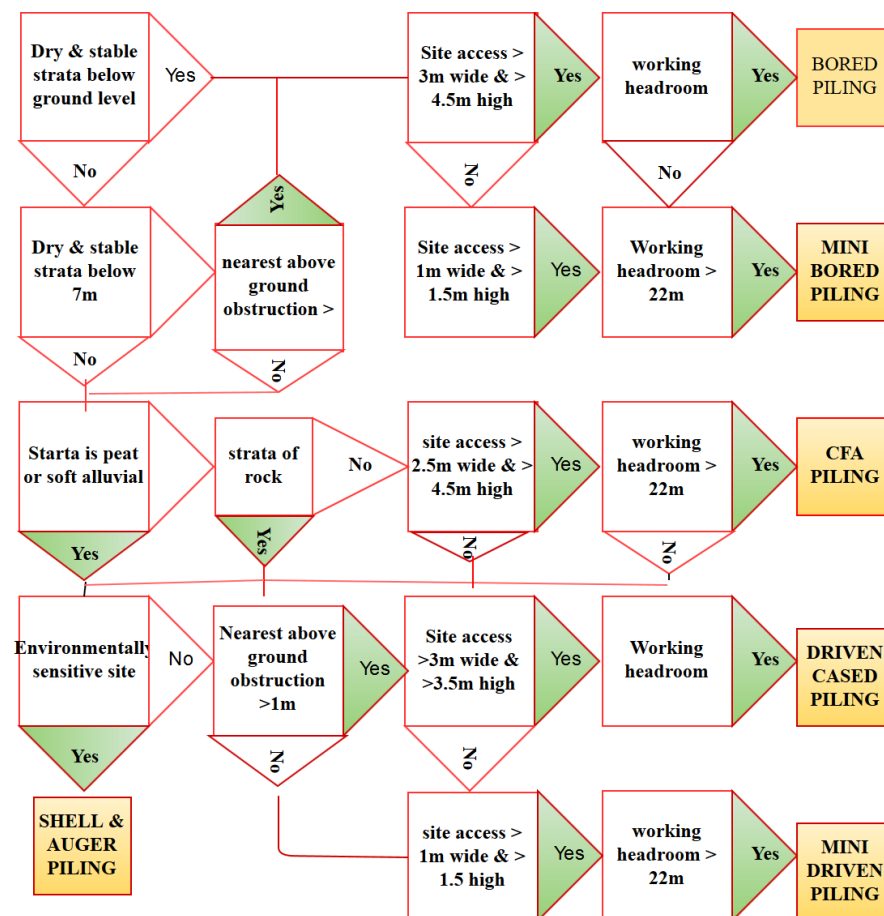


Figure 2.3: Flow chat for pile selection (Rao, 2009)

2.3 Geotechnical Bearing capacity of piled foundations

The allowable pile capacity is the minimum of allowable structural capacity or allowable geotechnical capacity. Piled foundations derive its bearing capacity/resistance from its shaft and end toe. For shaft bearing pile, it is governed by the shaft area. Shear forces mobilized between the piles and soil while end-bearing pile are governed by mobilized end toe shear forces (Eriksson, et al., 2004). According to Swedish practice the geotechnical bearing capacity of shaft bearing pile (e.g. cohesion piles) is calculated based on the undrained shear strength of the soil and can be expressed as the summation of the shaft resistance and end resistance. Swedish Commission on pile Research, recommends calculation of bearing capacity of a shaft bearing pile according to Equation (2.1). In long pile, the end bearing capacity is small compare to the shaft bearing capacity and often ignored in the calculation.

$$R_d = \frac{1}{\gamma_n} \int_{L_p} \frac{\alpha}{\gamma_{ma}} \cdot \frac{\theta}{\gamma_{m\theta}} \cdot \frac{c_{uk}}{\gamma_{mcm}} dz + \frac{N_{cp}}{\gamma_{mNcp}} \cdot \frac{A_s}{\gamma_{mAs}} \cdot \frac{c_{uk}}{\gamma_{mcs}} \quad (2.1)$$

Where:

- R_d = the bearing capacity of pile (designed value) [KN]
- L_p = the length of the pile [m]
- α = adhesion factor [-]
- θ = circumference of the pile [m]
- c_{uk} = undrained shear strength of the soil (unreduced) [KPa]
- N_{cp} = bearing capacity factor for pile toe [-]
- A_s = area of the pile section at the toe [m²]
- γ [-] = partial factors [-]

According Varanasi Rama Rao, 2009, factors influencing pile capacities are as follows,

- The surrounding soil
- Installation technique like driven or bored
- Method of construction (pre-cast or cast in situ)
- Spacing of piles in a group
- Symmetry of the group
- Location of pile cap i.e. above or below soil
- Shape of the pile cap, etc.
- Location of pile in the group and
- Drainage conditions in soil

2.4 Instrumented pile

Complex nature of soil and its variation in places, make it difficult to theoretically determine actual bearing capacity of pile and its behaviour with surrounding soil. Determination of the actual bearing capacity and behaviour of pile-soil interface demand field test. In deep foundation involving piles, instrumented piles are introduced to determine geotechnical bearing capacity, settlements, pore pressure, inclination and pile-soil interface behaviour. Figure 2.4 shows possible measurements during static testing. Instrumentation equipment are used to measure different parameters base on the aim of test study. Optical fibre sensing, extensometer, strain gauge and vibrating wire are used in measurement of strains.

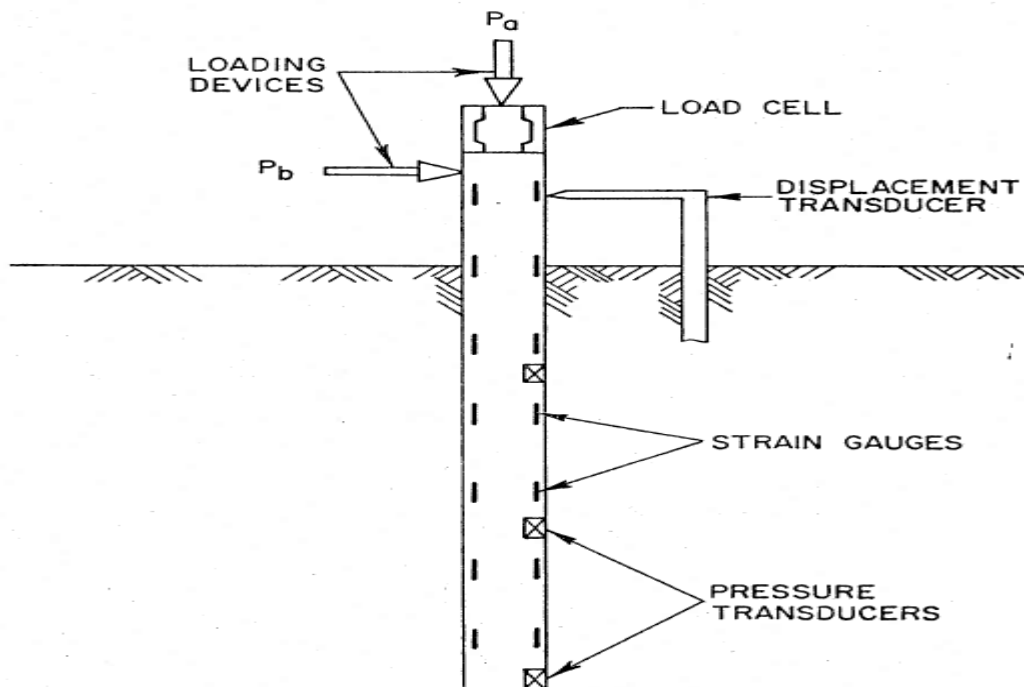


Figure 2.4: Possible measurements during static testing (Hirsch, Coyle, Lee L. Lowery, & Charles H. Samson, 1970)

The equipment is fragile and sensitive, hence proper installation of each are needed. Each of strain measurement equipment has its advantage and disadvantage.

Optical fibre

Optical fibre sensing that allows continuous strain measurement along the full length (up to 10km) when properly installed with Brillouin Optical Time-Domain Reflectometry (BOTDR). Optical fibres can measure both axial and lateral deformation by measuring strains from a single optical fibre placed along two sides of structure's plane. It is fragile and care must be taken when installing it and pile if driven method is to be used. Local features like cracking are often detected in pile (Mohamad, Soga, & Bennett, 2009). The optical fibre sensing has been successfully used in two different techniques; fixed-point-method for load bearing pile and end-clamped technique for secant-piled wall. Figure 2.4 show a configuration of optic fibre with BOTDR.

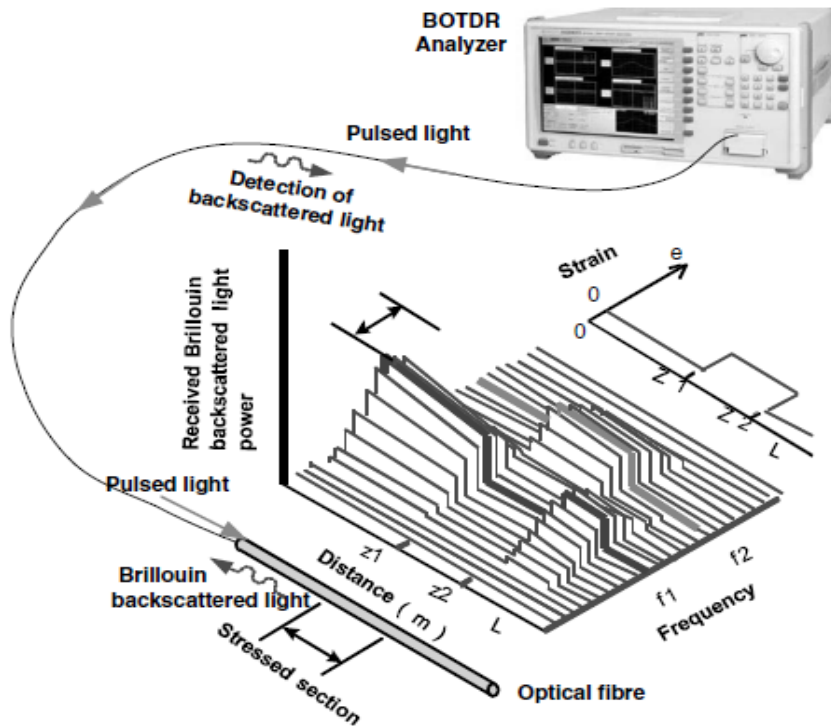


Figure 2.5: Optical fibre with BOTDR (Mohamad, Soga, & Bennett, 2009)

Vibrating Wire

Vibrating Wire Rebar Strain Gauges are used in monitoring the stresses in reinforcing steel in concrete structures, such as bridges, concrete piles and diaphragm walls. Figure 2.5 shows the components of vibrating wire. The strain meter comprised of a length of high strength steel, bore along its central axis to accommodate a miniature vibrating wire strain gauge. The measurement of load or stress is made with a data logging system. Strain meters are robust, reliable and easy to install. It is not easily effected by moisture and cable length. However, unlike the optic fibre, takes measures strain within a point. Hence, when installed location and serial numbers of all instruments are noted.

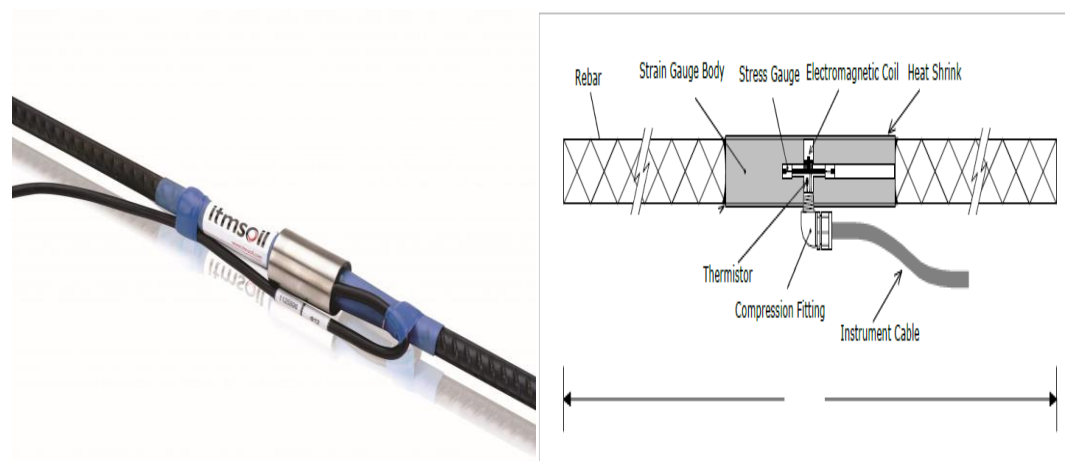


Figure 2.6: Vibrating wire rebar strain gauge and its components (Kim Malcolm, 2014)

Extensometer

Is pile instrumentation equipment used in measurement of soil and rock along a single axis. They are of different types, Rod extensometer, magnet extensometer, Sondex,

Borros Anchor settlement point, Settlement hook, Soil strain meter and Tape extensometer. Each type is used data required.

Its applications are as follows;

- Monitoring of settlement in excavations, foundations and embankments.
- Monitoring movements in rock slides, walls and abutments
- Monitoring subsidence above mines and tunnels
- Monitoring consolidation of soil under embankments and surcharges
- Monitoring compression of piles and soil under piles
- Monitoring spread in embankments and
- Monitoring convergence in underground openings, such as tunnels.



Figure 2.7: Extensometer

2.5 Pile Installation

Piles are installed either by direct displacement of soil or removal of soil and placing of the element in the bored hole. Piles installed in a group may fail as individually or as a block. Piles often fail individually when installed at large spacing (Sew & Meng, 2017).

Piles are installed with either of the following methods:

- Diesel/hydraulic/Drop hammer driving
- Jacked-In
- Prebore then drive
- Prebore then jacked-in
- Cast-in-situ pile

The pile life cycle commences with the installation of the pile. Displacement method in soft soil generate complex kinematic, resulting in large distortions of soil surrounding the pile shaft (Yanne, 2016). The current states of the soil-pile interface induced by the installation governs immediate and future behaviour of the pile foundation (Jardine & Lehane, 1994).

The method of installation of pile elements, contribute immensely to its future cycle. Displacement piles can be installed either by pile jacking or pile driving through heavy blows from hammer on pile head, forcefully driving it down the soil strata. Each method

of displacement pile installation has its pros and cons. Pile driving technic exert larger disturbance than jacking due to cyclic loading and unloading from the stress wave propagation from hammer blows. The stress wave in pile driving generate tensions loads which causes cracks to concrete, leading to reduction in stiffness, exposure of steel reinforcement to corrosion agents (Gebreselassie & Berhane, 2006).

Pile driving process, disturbs the soil at toe, pushes it downwards and displaces it's laterally. This installation process cause restructuring of the soil texture and stress history of the soil around the pile, hence forming a new soil-pile interface stress which governs the behaviour of the pile. For clays of very low permeability, the volume is relatively constant during installation (Claes, 2012). The total stress in the soil increases as soils are pushed downward and displace laterally. According to Randolph and Gourenvenec 2011, the increase is mainly due to the changes in the pore water pressure during undrain penetration, which tend to adsorb the force of blows from the hammer. However, as discuss in the pile history above at a stage in the pile history the excess pore water dissipates and the stress is transferred to the soil skeleton resulting to consolidation of the soil.

As the pile is forced downwards into soil, the total stress and the excess pore water pressure far above the pile toe reduces until they reach equilibrium, where there exist relative movement between soil-pile interfaces. Work of different author on different clays have found this limit to vary, According to Yannie Jorge 2016, Lehane and Jardine on Bothkenner and Saint-Alban clays studies found it to be around 15D from the pile toe and Roy et al. (1981) found it to be around 8.5D.

2.5.1 Pile Installation Requirements

Pile installation process and method of installation are as important as the selection and design of the pile. The rate of penetration of the piled during installation had a marked influence on the skin friction that could be mobilized during installation (Jardine & Richard, 1991).

To avoid damages to the piles, during selection and design, installation methods and installation equipment should be considered.

If installation is to be carried out using pile-hammer, then the following factors should be taken into to consideration:

- The size and the weight of the pile
- The driving resistance which has been overcome to achieve the design penetration
- The available space and head room on the site
- The availability of cranes and
- The noise restrictions which may be in force in the locality (The constructor, 2017).

2.6 Stages in Pile Foundation History

Pile interact with surrounding soils is of three main phases, installation, equalization and loading stage (Mar151). The vertical effective stress proportional to depth, prior to installation of pile, the vertical effective stress correlate with the horizontal as in the Equation2.2. The schematic Figure of pile – pore water - soil displacement process as in Figure (2.8).

According to Bond and Jardine 1991, at the installation phase, outward displacement of soil occurs leading to formation of residual shear plane between the soil and pile

surface. This process results to increase in mean total stress, which is accommodated by the corresponding increase in excess pore pressures. The process is regarded as undrained, hence there is no volume change (Ottolini, Dijkstra, & Tol, 2015). Equalisation stage commences initial settlement in pile history. The increase in excess pore pressure due to installation dissipates gradually towards the far field over time (Jardine & Lehane, 1994). And pore pressure at equalisation process at time zero equals the sum of the initial and incremental ($u_i = u_o + \Delta u$) (Yanne, 2016)). Due to dissipation of the pore pressure, the mean effective stress changes and initial settlement occurs around the pile. Leading to the decrease of the mean total stress as the soil contracts away from the pile resulting to increase in soil strength. At loading phase imposed loads on the pile head is transferred to the soil, hence increase rate creep settlement.

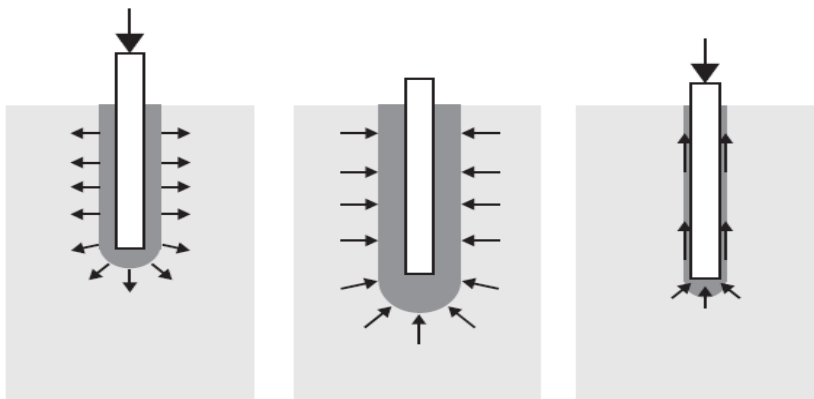


Figure 2.8: A schematic diagram of stages in piled foundation history, installation process (left), Equalization (centre) and loading (right) (Ottolini, Dijkstra, & Tol, 2015)

2.7 Settlements and Consolidation theory

When soil is loaded, it undergoes settlements in three components according to the Equation 2.5 (Holtz & Kovacs, 1981).

$$S_t = S_i + S_c + S_s \quad \dots\dots (2.5)$$

Where S_t = total settlements

S_i = immediate settlements

S_c = Consolidation settlements

S_s = secondary consolidation or creep settlements

The immediate settlements are the immediate deformation observed upon instant loading of soil. Consolidation settlement is a time dependent deformation occurring in soil with low permeability due to pore water seepage causing increase in the effective stresses in the soil. Creep settlement is also a time dependent settlements, which occurs at relatively constant effective stress.

2.7.1 Consolidation settlements

Soil consolidation can be like to spring analogy as illustrated in Figure. A saturated soil is modelled as a water-filled cylinder containing a spring that is connected to a piston (Kovacs & Holtz, 1981).

In the model the spring stands for the soil skeleton and the stress induced in it from the applied load is equivalent to the effective stress. While the pressure in the water represent the pore water pressure in the soil, u , the opening at the valve represent the pore sizes in soil structure. In Figure 2.6a, there is no flow of water through the valve, on add load the pore pressure increases as equivalent to the load applied. As more water flows out from, the load is transferred to the spring and a vertical deformation occurs Figure 2.9b. The rate of deformation depends on flow rate governed by the load applied and pore sizes in the soil. At certain time, spring again be in equilibrium with overburden pressure and water stops to flow from the cylinder, Figure 2.9c. The transfer of increase in pore pressure due to applied load to effective stress is as in Figure 2.10

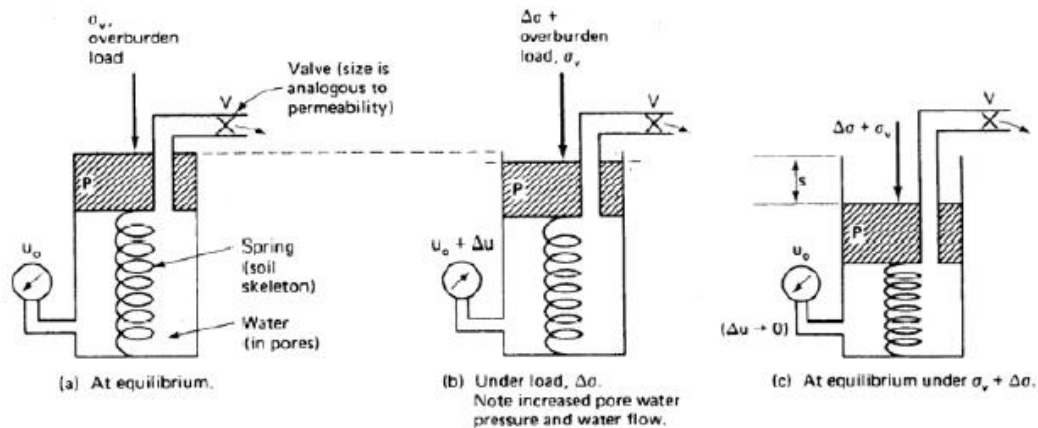


Figure 2.9: the spring analogy applied to the consolidation process.

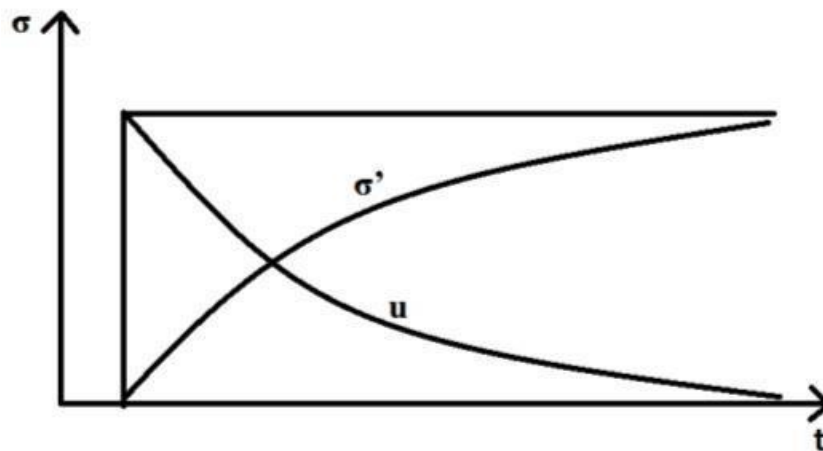


Figure 2.10: Transition of load from pore water pressure to effective stress during consolidation

Mathematical model of consolidation

Determination of magnitude and degree of consolidation, (Terzaghi, 1943) developed a mathematical model based on the following assumptions:

1. The soil is homogeneous.
2. The soil is fully saturated.
3. The soil particles and water are incompressible.
4. Compression and flow are one-dimensional.
5. Strains are small.
6. Darcy's law is valid at all hydraulic gradients.
7. The coefficient of permeability and the coefficient of volume compressibility remain constant throughout the process.

8. There is a unique relationship, independent of time between void ratio and effective stress.

The consolidation process can be described with Equation 2.6

$$\frac{\partial u}{\partial t} = \frac{M}{\gamma_w} * \frac{\partial}{\partial z} * \left(k * \frac{\partial u}{\partial z} \right) \dots \dots \dots (2.6)$$

Where;
 u = pore pressure (KPa)
 T = time (s)
 M = odometer modulus (KPa)
 γ_w = unit weight of water (KN/m³)
 K = permeability (m/s)
 Z = depth (m)

Since, $k = 0$; Equation 2.7 becomes

$$\frac{\partial u}{\partial t} = C_v * \frac{\partial^2 u}{\partial z^2} \dots \dots \dots (2.7)$$

Where $C_v = M * \frac{k}{\gamma_w}$ [m²/s]

C_v = coefficient of consolidation, which determines the speed of consolidation process. Since k , M , and γ_w are assumed to be constant in model, C_v is constant during consolidation (Knappett & Craig, 2012). To simplify Equation 2.8, time factor T_v is used when calculating consolidation settlements.

$$T_v = C_v * \frac{t}{d^2} [-] \dots \dots \dots (2.8)$$

Where t = time (s) and d = drainage distance (m)

When T_v is known, it is possible to find the average degree of consolidation U_v by using graphs as shown in Figure 2.11. The different curves represent the relationships between U_v and T_v for different initial variations of excess pore water pressures due to loading.

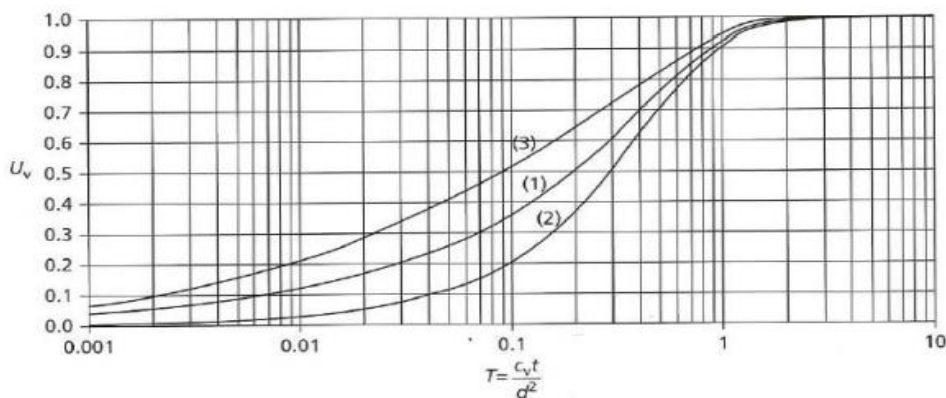


Figure 2.11: Relationships between average degree of consolidation U_v and time factor T_v for different initial variations of excess pore pressures (Knappett & Craig, 2012)

2.7.2 Settlement of piled foundations

According Claes A. 2009, settlements in piled foundation due to imposed loads and negative skin friction can principally be describe as sum of three main components;- **immediate/primary** consolidation associated with dissipation of excess pore pressures, **secondary consolidation** associated with rearrangement of the particles and **creep** associated with shear stress-strain. The amount of settlement at any point along x-axis in pile can be determined by summation of compression in pile above the point, differential movement between the pile and soil surface (slip) at the point and settlement below that point. As express in Equation 2.12.

$$\sum S = S_1 + S_2 + S_3 \dots \dots \dots (2.9)$$

Where; S_1 = compression in the pile elements

S_2 = slip between the piles and the ground

S_3 = settlements in the ground.

The above pile settlement components can be calculated with the following formulae,

$$S_1 = \frac{(Q_{wp} + \xi Q_{ws})L}{A_p E_p} \dots \dots \dots (2.10)$$

$$S_2 = \frac{q_{wp} D (1 - \mu^2) I_{wp}}{E_s} \dots \dots \dots (2.11)$$

$$S_3 = \frac{Q_{ws} D (1 - \mu^2 s) I_{ws}}{\rho L E_s} \dots \dots \dots (2.12)$$

Where,

Q_{wp} = load carried at the pile tip resting on the soil, under working load condition

Q_{ws} = load carried by skin friction under working load condition

L = Length of the pile

E_p = Modulus of elasticity of pile material

A_p = Area of cross section of pile material

Q_{wp} = load at pile tip per unit area

μ = poisons ratio of the soil

$I_{wp} I_{ws}$ = influence factors

Due to high stiffness of pile element resulting to small value of the compression, it is often ignored (Claes, 2012). Slip displacement between the pile-soil interfaces is small, normally less than 5 mm, if there is no friction failure. Hence, with the determination of the point of no friction other components can be obtain with aid of neutral plane concept.

2.8 Negative skin friction and Neutral Plane

After pile installation, remoulding of soil occurs leading to settlement process causing down drag. This phenomenon is called negative skin friction (Claes, 2012). The negative skin friction is proportional to the effective overburden stress in the soil (Fellenius B. H., Negative skin friction and settlement of piles, 1984). The constant of proportionality is called beta-coefficient, β , a function of earth pressure coefficient in the soil K_s , times the soil friction, $\tan \phi'$, times the ratio of the wall friction, $M = \tan \delta'$

$\tan \phi'$. As in Equation 2.13. In pile history, a stage exists when action effect due to the ongoing process changes into friction strength (resistance). The depth at which on friction stress and slip between pile-soil interface is zero is known as **neutral plane**.

$$q_n = \beta \delta'_v = MK_s \tan \phi' \dots \dots \dots (2.13)$$

Below plane, settlement in pile and ground occur uniformly. In cases of no settlement at any depth, implies that there is no additional down drag below the depth, hence a zone of equal strain in the ground and the pile occurs. The stresses are governed by stiffness of pile and soil. Figure 2.8, shows action in pile due to imposed loads. The action effect in the pile at a depth z can be obtained with Equation 2.14 (Claes, 2012). Action effects increases down long pile, while resistance increases upwards. Figure 2.12, illustrate forces in pile element, relation between the pile and soil and force diagram due to the action and resistance effect in pile respectively

$$E = Q + \int_0^z f_m dA \dots \dots \dots (2.14)$$

Where: Q = the loading of the pile [KN]
 f_m = the shaft resistance per shaft unit area [KPa]
 A = the shaft area [m²]

Similarly the resistance R at depth z can be obtained with Equation 2.4.

$$R = R_{toe} + \int_z^{L_p} f_m dA \dots \dots \dots (2.15)$$

Where: R_{toe} = the resistance at the pile toe [KN]
 L_p = the length of the pile (m)

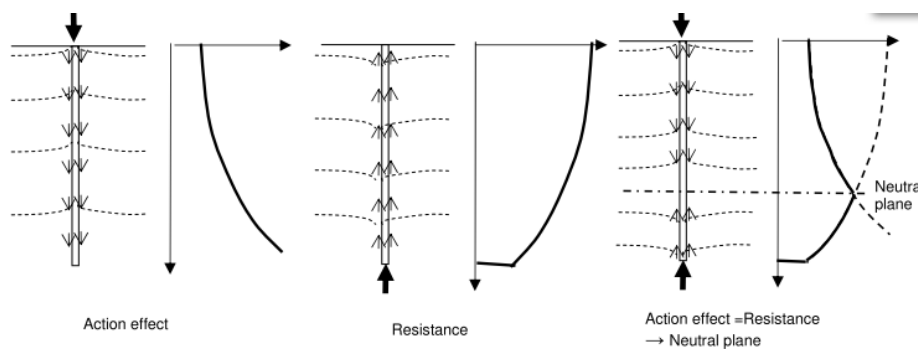


Figure 2.12: Action effect/Resistance interaction on pile foundation (Claes, 2012)

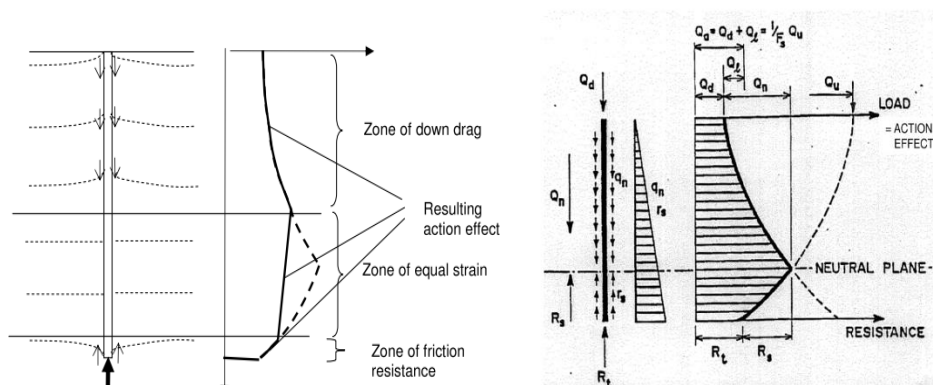


Figure 2.13: illustration of neutral plane and shear forces in pile (Claes, 2012)

The negative skin friction reduces pile carrying capacity which lead to deformations in superstructure (Sew & Meng, 2017). According Sew & Meng, 2017, the following preventive measures should be observed to reduce the effects of negative skin friction:

- Free filling should be avoided
- Carry out surcharging
- Sleeve the pile shaft
- Slip coating
- Structural capacity should be reserved for negative skin friction
- Allow for larger settlements in design.

2.9 Piled foundation Analysis

Scholars in geotechnics field have develop so many theoretical methods to analysis behaviour of single piles and pile groups, in different approach. Zhang et al. (2012), classified these various theoretical methods into five categories as follows:

(i) *The theoretical load-transfer curve method* by Kraft et al. 1981; Xiao et al. 2002; Zhang et al. 2010a, adopt load transfer function to describe the relationship between the unit skin friction transferred to the surrounding soils and the pile-soil deformation behaviour in each soil layer;

(ii) *The simplified analytical methods* by Randolph and Wroth 1979; Lee 1993; Guo and Randolph 1999, consider vertical displacement of the soil induced by the shaft resistance as a logarithmic relationship of the radial distance as a logarithmic relationship of the radial distance away from the pile shaft;

(iii) *The boundary-element method* by Mandolini and Viggiani 1997; Mendonca and De Pavia 2000; Ai and Han 2009. Employs either load-transfer functions to capture the interaction response or elastic continuum theory to simulate the soil mass response.

(iv) *The finite element method* by Sheng et al. 2005; Comodromos et al. 2009; Said et al. 2009. Which considers to be one of the most powerful approaches for the analysis of the behaviour of single piles or pile groups, however, it is not commonly used in practice because of its high computational requirements;

(v) *The variation approach* by Shen et al. 1997, 1999, 2000 which has been used recently in the analysis of piled raft foundations. The shaft resistance degradation and skin friction softening with increase in displacement were not properly taken into consideration in those analysis (Zhang & Zhang, 2012).

According to Zhang et al. 2012, Zhao et al. 2009; Zhang et al. 2010b, 2011a, 2011b, in practice investigated shaft resistance and observed skin friction softening with increasing displacement. Hence, adopt two models approach in analysis of single piled to consider the skin friction softening and bilinear model. In analysing load-settlement relationship developed at the pile end in practical application came up with a model called **a simplified nonlinear approach for single pile load-settlement analysis**. That will be discuss further in the next Section and determination of the parameters for the numerical computation.

2.10 Single pile load-settlement analysis.

In Zhang, et al. 2012 single piled load transfer analysis, two models were combined - a *softening nonlinear model of skin resistance* and a *bilinear base load-displacement model*. The models were employed in analysis of the single piled to in cooperate the practical field observations. In comparing theoretical results of the proposed combined model with field test on a single pile, the calculated and measured results were satisfactory.

2.10.1 A softening nonlinear model of skin resistance

The simple softening model deals with the de gradation behaviour between the skin friction and pile-soil relative displacement developed at pile-soil interface. The skin friction and corresponding shear displacement shows a softening characteristic when skin friction is fully mobilised Zhang et al. 2012. The shaft shear stress and shear displacement relationship illustrated graphically in Figure 2.8.

At first, pile-soil friction increases nonlinearly with increasing pile head load up to a point when the pile-soil relative displacement reaches *maximum value* S_{su} , and unit skin friction attain its *ultimate value*, T_{su} . At this, the unit skin friction starts to decrease with increasing displacement along the pile-soil interface. When the relative shaft displacement goes to infinites ∞ , the skin friction remains at a residual value, T_{sr} . Ratio of the residual unit skin friction to the limiting unit shaft resistance is defined as β_s . It has been found to be between the ranges 0.83 – 09.7 for bored piles (Zhang & Zhang, 2012).

Fig. 2.14. Relationship between skin friction and relative shaft displacement at the pile-soil interface (Zhang et al. 2012).

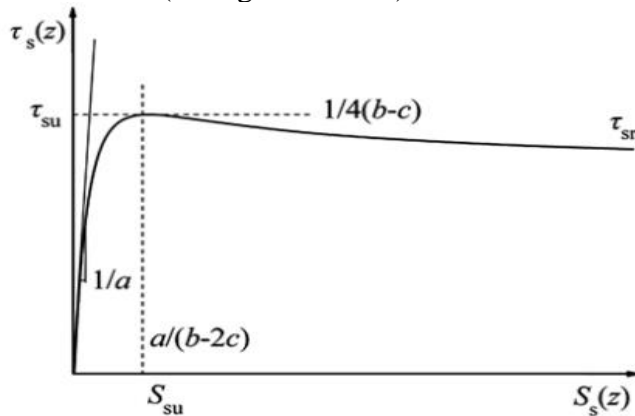


Figure 2.14: Assumed relationship between skin friction and relative shaft displacement at the pile soil interface (Zhang & Zhang, 2012).

The relationship at any given depth along the pile shaft can be approximated with the Equation 2.16

$$T_s(z) = \frac{S_s(z)[a + cS_s(z)]}{[a + aS_s(z)]^2} \dots \dots \dots (2.16)$$

Where $T_s(z)$ = shaft shear stress at given depth, z ,

$S_s(z)$ = relative displacement along the pile-soil interface at a given depth, and a , b and c are empirical coefficients.

From (Zhang & Zhang, 2012)), values of the parameters are determined from Equations below,

$$S_{su} = \frac{a}{b - 2c} \dots \dots \dots (2.15)$$

$$T_{su} = S_{su} \frac{[a + cS_{su}]}{[a + bS_{su}]} = \frac{1}{4[b - c]} \dots \dots \dots (2.16)$$

$$T_{su} = \lim_{s(z) \rightarrow \infty} \frac{(Ss(z)[a + cSs(z)])}{[a + bSs(z)]^2} = \frac{c}{b^2} = \beta s T_{su} \dots \dots \dots (2.17)$$

$$b = \frac{1 - \sqrt{1 - \beta s}}{2\beta s} \dots \dots \dots (2.18)$$

$$c = \frac{2 - \beta s + 2\sqrt{1 - \beta s}}{4\beta s} \frac{1}{T_{su}} \dots \dots \dots (2.19)$$

$$a = (b - 2c)S_{su} = \frac{\beta s - 1 + \sqrt{1 - \beta s}}{2\beta s} \frac{S_{su}}{T_{su}} \dots \dots \dots (2.20)$$

The value of S_{su} is determined experimentally or by back-analysis of field load test results. The factors affecting the interface behaviour of actual pile at a site such as construction methods, pile types, soil types, stratigraphy and loading procedure influence the magnitude of the shaft S_{su} .

2.10.2A bilinear base load-displacement model

The model describes the load- displacement response develop at pile end. It is drive from test results and analytical solution from Zhang et al. 2010a. The load-displacement relationship at the pile base is assumed to follow a bilinear model as in Figure 2.11. The pile base settlement due to mobilised load at the base are obtained from Equation 2.21

$$T_b = \begin{cases} k_1 w_b & w_b < S_{bu} \\ k_1 S_{bu} + k_2 [w_b - S_{bu}] & w_b \geq S_{bu} \end{cases} \dots \dots \dots (2.21)$$

Where T_b = unit end resistance
 w_b = pile end settlement
 S_{bu} = pile end settlement related to the limiting end resistance in first stage
 k_1 & k_2 are compressive rigidity of the pile-tip in the first and second stage in Figure 2.15.

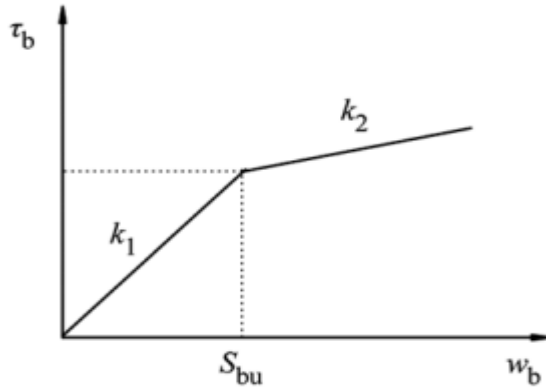


Figure 2.15: Assumed relationship between end resistance and pile-end settlement (Zhang & Zhang, 2012)

The values of k_1 and k_2 can be determined according equations 2.22 & 2.23 respectively as suggested by Randolph and Wroth (1978).

$$k_1 = \frac{4G_{sb}}{\pi r_o(1 - \nu_b)} \dots \dots \dots 2.22$$

Where G_{sb} and ν_b are the shear modulus and poison's ratio of the soil below the pile base, respectively.

According Zhang et al. 2010a, the value of k_2 can be approximated as in Equation 2.23

$$k_2 = \frac{\Delta P_t}{\Delta w_t - \left(\frac{\Delta P_t L}{E_p A_p}\right)} = \frac{k_1}{1 - \left(\frac{k_t L}{E_p A_p}\right)} \dots \dots \dots 2.23$$

Where ΔP_t = increased in load at pile head when the settlement at the pile base is larger than the limiting pile end settlement of the first stage of the T_b-w_b curve;

Where: Δw_t = is the increased settlement at the pile head induced by ΔP_t

L = pile length

E_p = pile elastic modulus

A_p = cross sectional area of the pile element

k_t = ratio of the load increment to the settlement increment at the pile head, i.e. $k_t = \Delta P_t / \Delta w_t$.

S_{bu} is determined experimentally or by back-analysis of field load tests results. Its magnitude is influenced by the construction method, condition of the soil under the pile tip and stratigraphy

3 Analysis Algorithms

A single piled analysis approach was adopted used in the study. A Zhang method for load-settlement analysis of a single pile (Load-Transfer method) embedded in layered soils and neutral plane approach. Algorithms of each method are discussed in next Sections.

3.1 Neutral plane approach

Is a method of determination of the neutral plane based on assumption of ongoing settlement, caused by external actions such as ground water lowering or creep deformation. A plane of frictionless is determined where the action effect turns to resistance and settlement in the pile-soil becomes uniform. (Mats Ekenberg & Lijenfldt, 2015)

With Equation 3.1 and 3.2 respectively the characteristic bearing capacity R_k and design value of bearing capacity, R_d where obtained

$$R_k = \alpha * C_{uk} * A_m \dots \dots \dots (3.1)$$

$$R_d = \frac{1}{\gamma_{rd}} * \left(\frac{R_k}{\gamma_m * \gamma_n} \right) \dots \dots \dots (3.2)$$

Where γ_{RD} = model factor, γ_{nm} = Partial factors for shaft resistance, γ_n = partial factor for safety class *SKI*.

Undrain shear strength, C_{uk} at depths $Z_i - Z_n$ along the pile length, action effect from the pile head to toe and resistance from toe to pile head were calculated graph of $E - z$ and $R - z$ plotted.

3.2 Load – Settlement analysis method

This approach was used to study load transfer, elastic deformation in the piled element and likely settlements due to the imposed load at the pile head. Three (3) scenarios where considered; (a) behaviour of piled foundation as function of pile head load at time zero (0), (b) Pile Stiffness effects and (c) Down drag effects.

The two models proposed Zhang et al. (2012), discussed in previous Sections in Chapter 2 with parameters in Table 3.1. A single pile element of 65m length was used. The pile element was divided into seven (7), segments of 10m each and the final lap is 5m, as shown in Figure 3.1.

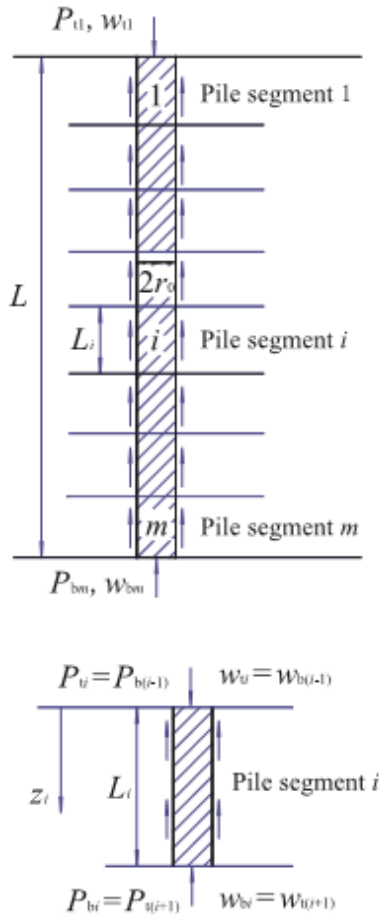


Figure 3.1: A single pile embedded in layered soil

At start of the analysis, a constant pile head load P_{t1} , of 3000kN was assumed on pile head, based on the estimate of the load test to be carried out in field, assumed to produce a corresponding small pile head settlement of 0.052 m. considering segment 1 of the pile element, the elastic deformation, S_{c1} , was calculated with Equation4.

$$S_{c1} = \frac{P_{t1}L_1}{A_p E_p} \dots \dots \dots (3.1)$$

Where: L_1 = length of pile segment 1, I.e. 10m
 A_p = pile cross section
 E_p = elastic modulus of pile, 300GN/m²
 P_{t1} = constant pile head load.

The vertical movement w_{c1} , at the middle pile segment 1 of the pile with Equation3.2

$$w_{c1} = w_{t1} - 0.5S_{c1} \dots \dots \dots (3.2)$$

With the mathematical model of a softening nonlinear model of skin resistance, Equation2.3 of the shaft shear stress T_{s1} , pile-soil interface in segment 1 was determined by substituting Equation3.2 into the model. The total skin friction of pile segment 1, T_1 , was determined with Equation3.3.

$$T_1 = 4BL_1t_{s1} \dots \dots \dots (3.3)$$

Where; B is the breadth of x-section of square pile element.

The mobilized base load of pile segment 1, P_{b1} , was calculated with Equation3.4

$$P_{b1} = P_{t1} - T \dots \dots \dots (3.4)$$

Then the average axial load in the pile segment 1, P_1 , was calculated with Equation3.5

$$P_1 = \frac{P_{t1} + P_{b1}}{2} \dots \dots \dots (3.5)$$

With the values the modified compression of pile segment 1, $S'c1$ determined with Equation3.6

$$S'c1 = \frac{P_1 L_1}{A_p E_p} \dots \dots \dots (3.6)$$

The modified compression $S'c1$, of pile segment was compared with initial computed elastic deformation of pile segment 1, $Sc1$. The value of the assumed settlement on pile head was adjusted and 4 steps Equation3.2 to Equation3.6 iterated until difference between modified compression and initial elastic compression agree with a specific tolerance of 1×10^{-6} m as recommended by Zhang al et. 2012.

End displacement of pile segment 1, wb , was determine with the Equation3.7

$$wb1 = wt1 - s'c1 \dots \dots \dots (3.7)$$

The mobilized base load and end displacement of the segment 1 were used as pile head load and pile head settlement respectively for next segment immediately below it and so on till the last segment of the pile element, 5m. Thereafter, step 3 Equation3.1 to Equation3.7 procedure was repeated from Equation3.1 in segment 1 until the pile end settlement of a certain pile segment i , is within the assumed tolerance, or the mobilized base load of a certain pile segment is within an assumed tolerance.

Since the mobilized base settlement of pile segment i , is larger than the assumed small value of 1×10^{-6} m, and the base movement of pile segment $i+1$ is less than $1 \times 10 \times 10^{-6}$ m, the total skin friction or sum of the skin friction of the pile length was approximately estimated by Equation3.8.

$$T = T1 + T2 + \dots + Tm + Pbm \dots \dots \dots 3.8$$

In a case where the mobilized base settlement of pile segment m , is larger than the assumed small value of 1×10^{-6} m, the mobilized base load will be computer with Equation2.10 and sum of skin friction will be calculated with Equation3.9.

$$T = T1 + T2 + \dots + Tm + Pbm \dots \dots \dots 3.9$$

Where P_{bm} is the mobilized base load at pile segment m , calculated from Equation2.10.

Procedures above from step 2 Equation 3.1 to Equation 3.8/9 were repeated, by using a large pile head settlement value, w'_{t1} , to obtain another sum of the total skin friction and mobilized base load, T' .

Procedures above from step 2 Equation 3.1 to Equation 3.8/9 were repeated again using an average pile head settlement of the two previous procedures, $w_t^{ave} = (w'_t + w_{t1})/2$. To obtain sum of total skin friction and mobilized base load, T^{ave} .

T^{ave} was compared with the load at pile top ($P_{t1} - T^{ave}$) to ensure it was within the specific tolerance 1×10^{-6} m as recommended by Zhang et al. 2012 or the condition $(T^{ave} - P_{t1})(T - P_{t1}) < 0$. If $(P_{t1} - T^{ave})$ is within the specific tolerance 1×10^{-6} m, the value w_t^{ave} is the settlement at the pile top caused by the pile head load P_{t1} .

The procedure from step 3 Equation 3.1 was repeated using different assumed load level at the pile top, P_{t1} , to obtain series of load – settlement responses developed at the pile head.

In scenario 2 –down drag effect. The down drag effect was incorporated as form of settlement at different depth in the soil. Settlement measurements around the construction site over a period of five (5) years within soil were superimposed at different segment of pile i.e. Equation 3.2 minus the settlement value. To study load – settlement behaviour of the pile due to the oncoming ground settlement in the area.

4 Case Study

In this report three case studies were considered. For pile analysis, E45 project Lilla-Bommen-Marieholm tunnel foundation, discussed in details in the next Section. For investigation of installation effects on instrumentation, reports on pile instrumentation works done in past in Sweden were studied, which will be discussed in later Section.

4.1 E45 project: Lilla-Bommen-Marieholm tunnel foundation

Over the years the Lilla-Bommen-Marieholm section of E45 highway has evolved from one stage to order as city grows and transport demands increase. From mere farm lands in 1790 to city outlook in 1900's, Figure 3.1. The Marieholm was an island in the Gota Alv River until the second half of the 19th century. Industrialization of Marieholm commenced around year 1900 when several large industries were established, including Slakthuset in year 1903 (Lönnroth, 2000). Since then, it has continued to be an industrial area with several large infrastructural projects evolving. A railway bridge was built in southern part in 1909 (Medin & Johanna, 2015) and E45 highway crossing the area from north to south was built in the late 1960's.



Figure 4.1: Evolving stages of study area

The city demand for sustainable and efficient transport system in recent years have necessitated the reconstruction of the sections of the highway. The proposed new plan, lowers the E45 road approximately 6 meters between city Service Bridge and east of Falutorget, about 800 meters. The western part between the city service and Torsgatan to constitute tunnel while the part from Torsgatan and up to Falkenberg to be submerged in future. Leading to construction of new bridges across Kampegatan.

In the tunnel section, there will be a high-rise building and retaining walls. In its foundation, will be piles installed in the soft clay.

A total of about 250 000m displacement floating concrete piles. Of which four (4) of its will be instrumented piled foundation, for study of piles behaviour and capacity for future purposes. Figure 10a & b, shows location and current state of the study area.



Figure 4.2: Overview map with tunnel section marked in orange and ongoing construction at tunnel site (Daniel Hägerstrand, 2017)

4.1.1 Topography and surface Conditions

The current area is an urban environment, which is mostly artificial hard surfaces. The level of the surrounding area is between the height of +1.5 to + 2.0 along the proposed tunnel. The existing profile of road E45 is on level about -4. The level of the road E45 rises from Stadstjarnarebron up to about +2 at Holmen's regulation. The area around the Gullbergs that connects E45 with E6 at Tingstad tunnel. The ground surface is generally horizontal.

In and around the road, there are green areas with grass, trees and bushes. Ground level on green spaces is around level +2. Topography and surface conditions are also evident from models established in the project.

4.1.2 Geotechnical Conditions

Several geotechnical researches with advanced field and laboratory equipment were conducted in the study area in bid to understanding the geotechnical and hydrogeological conditions. The geotechnical and hydrogeological studies were performed by companies at different time as reported by Mats Ekenberg & Lijenfldt, 2015 in Markteknisk undersökningsrapport of the project. The report was made in accordance with conditions for application of geotechnical category 2 and 3 as demanded by Transport Administration's Technical for Geo Structures, TK Geo 13 (Mats Ekenberg & Lijenfldt, 2015).

4.1.3 Soil profile

The soil consists of deep layer of clay of 70m to 100m, with fill material approximately 0.5m to 2.5m. For analysis in this study, the depth of the clay was assumed to be 100m. The clay found in the area is typical Gothenburg clay, having water content around 65% to 85% and an undrained shear strength of 15 in the upper layers and increasing to 70kPa in a depth of 50m.

Oedometer and CPT test result from Chalmers laboratory (Mats Ekenberg & Lijenfldt, 2015), gives the OCR to be approximately 1.0. Hence, the soil is classified as normally consolidated. The in-situ stresses from the test boreholes is $0.8 \sigma'_c$ and settlements have been classified as creep settlement with a rate of 0.5 – 2mm/year (Mats Ekenberg & Lijenfldt, 2015). For the location of the borehole see appendix A1.

4.1.4 Soil Parameters

From soil test results of chosen boreholes near the location of instrumented pile, important soil parameters for piled foundation analysis was determined.

Unit weight - γ_{soil}

The unit weight of the clay within the tunnel section from the test boreholes close to location of instrumented piles is relatively constant with depth. Approximately 16 kN/m³ at the upper part of the soil profile. In the deeper layers, 17kN/m³.

Water content W_N and liquid limit W_L

The evaluated values of water content and liquid limit from boreholes UP02_ 03, UP03_10, 1_A, K1, 22001 and 22003 plotted against depth. The water content varies from 30% to 100% in the first 10m, below 10m it become slightly lower between 60% and 85%. The liquid limit varies less with depth compare to the water content with a value of 60% to 100% at first 10m and 60% to 80% at below 10m. Comparing the two, they are very close at all depth in the profile.

Pore water pressure – u

The groundwater table varies between 1m and 1.5m below the ground surface. The measured pore water pressure distribution and the hydrostatic pore pressure are plotted against depth. The groundwater level from CPT result is located at 1 meter below ground surface. The pore water pressure generally around 10kPa higher than hydrostatic pore pressure below a depth of 15m.

Undrained shear strength – C_{uk}

The undrained shear strength deducted from the CRS, CPT, DS and Triax test reported by Mats Ekenberg & Lijenfldt from different boreholes location along the tunnel section as shown in Appendix A.2. The undrained shear strength plotted against depths, shows a linear increase at greater depth of up to 95 meters. A linearization of the plotted values are as in Equation 4.1:

$$C_{uk} = \begin{cases} 15 \text{ kPa} & z < 4 \\ 15 + 1.08(z - 4) & z \geq 4 \end{cases} \dots \dots \dots (4.1)$$

4.2 Instrumented pile

For study of pile behaviour in E45 tunnel foundation, piles of cross section of 275 x 275mm were used. The concrete strength of the pile at 14 days is C60/75 strength. A total of 245 m out of 250 000 m piles in the project were instrumented. Giving four (4) piles of 65 m x 3 and 50 m lengths. For measurement of strain, vibrating wires were installed, see Figure 4.5. In 65 m and 50 m instrumented pile, a total of 20 and 16 numbers of vibrating wires were placed at five (5) and four (4) sections respectively along the pile with four (4) at each section.



Figure 4.3: Geokon vibrating wire on 1m sister bar used in instrumented piles

The vibrating wire were fixed to sister bar of high yield steel approximately 1 meter, well painted to reduced corrosion. The sister bar fastens to each side of reinforcement bar. In 65 m pile, vibrating wire where placed at 2m, 19.5m, 32.5m ,45.5m and 63m while in 50m pile at 2m, 19.5m, 32.5m and 48m respectively from top. The sister bar at 2m and 63m and 48m in each pile length where installed to measure strains at pile head and toe while others measures stain at middle of the pile. See appendix for the cross sections of the pile.

The cable from each layer of instrumentation where secure from pore water spillage with a flexible horse of 4 inch, Figure 4.6. The wires from each section of instrumentation will be placed in semi-circular pipe and fasten to concrete external surface.



Figure 4.4: Vibrating wires installed with flexible protective horse

Inclinators were installed at site to measure piles inclination and possible bend in pile as result of installation processes. Pore pressure gauge will also be installed to measure and control movement of pore water and pore pressures. Plastic sheet pile walls where installed around construction site to monitor pore water flotation and prevent undue subsidence around the project site. In the construction site, pile where installed at -12m, to reduce effects of waves from installation process, Figure 4.7. The instrumented piles

will be installed along the walls of tunnel, one at south and north walls and 2 at center wall.



Figure 4.5: Installed piles at construction site at depth of -12m

4.3 Skanska high-rise building, Lilla-Bommen/ Tolo Tvarled instrumented pile

In this Section, a study on report of an instrumentation works made on Skanska high-rise building as reported by Peter Claesson, Gunnar Holmberg, & Jan Romell, 2007 is presented. Its location, aim and objects, pile instrumented works on cohesion piles used in the foundation, result and challenges encountered with the instrumentation.

The building currently located at Lilla-Bommen area of Gothenburg, used as office complex is of 22 floors, popularly referred as lipstick. During its construction, eight (8) test piles were instrumented, settlements in building and surrounding area. The instrumentations were made in four (4) levels in each test pile, see Figure 4.8. In consideration of reliability for a long time with difficult conditions, a mechanical measuring system was used, in form of strain wire screwed to test pile surface as shown in cross section Figure 4.9 where used to measure displacements. At each level, four measuring strins were installed. Two on each side of the two sides of the pile as shown in x-section in Figure 4.7a. On each of the pile instrumented, some of the measurement points failed to measure after installation.

In the case of Tolo Tvarled instrumentation work, from the discussion with Per Ola, a structural engineer from Skanska AB involved in the instrumentation of the piles. The aim was to study the settlement in structure supported by the cohesion piles and load distribution due to down drag effect. In the instrumentation of the pile, the original plan was to install three (3) equipment ; optical fibre sensing, extensometer and strain gauge and at end compare the readings from each.

In the test pile, at construction phase of it (casing) steel pipe was placed at centre of pile through which instrumentations will be installed. At stage of installation, it was found that size of the hole made was not sufficient to install the three equipments proposed. However, two of it was forced into the hole. The extensometer and optical fibre was installed. At process of installation, the mirror in optical fibre broke and reading was only obtained from the extensometer.

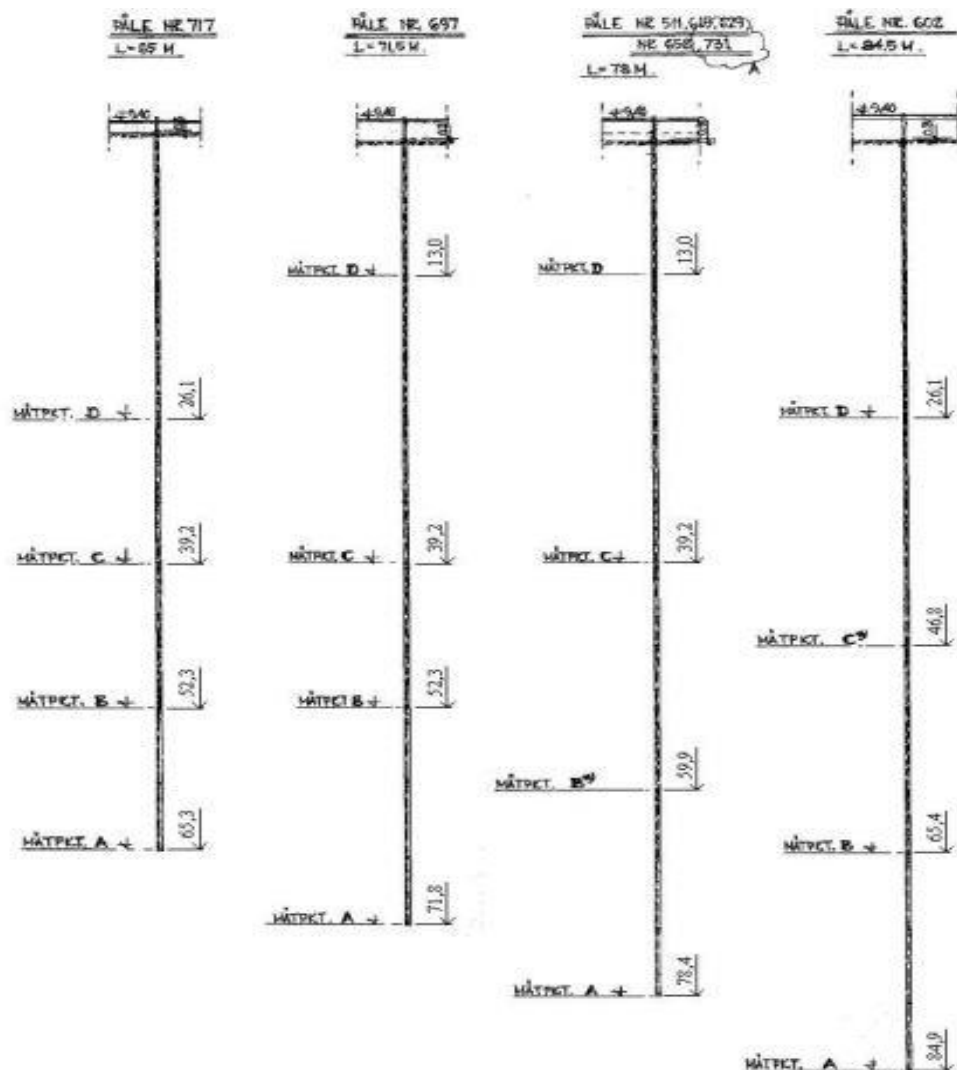


Figure 4.6: measuring points for instrumented piles (Mats Ekenberg & Lijenfldt, 2015)

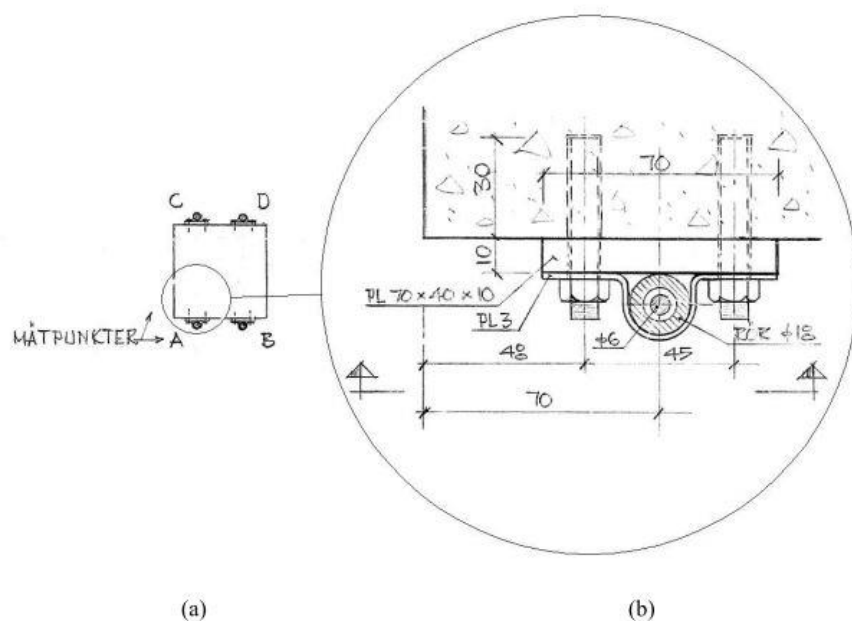


Figure 4.7: (a) Section through pile with four measuring tubes (b) Mounting detail for measuring tube

5 Results and Discussion

The results from the two methods and findings on effects of pile installation process on instrumentation are presented in this chapter.

5.1 Neutral plane Approach

In this Section, the results of analysis made with the neutral plane approach are presented. For the input data used and detailed calculation, see Appendix B1. From this analysis, the characteristic bearing capacity, R_k of the 65m pile is 3582 KN. In the calculation of action effect and resistance, 4m depth of fill was neglected, since in real situation, there may not be friction at that length because of holes likely to exist in the depth and will not contribute to skin friction experience by the pile.

Figure 5.1 and 5.2 shows the neutral plane estimate from action effect and resistance computation and strain distribution below neutral plane respectively. From the analysis, as shown in Figure 5.1, the neutral plane is at 32m (i.e. 28+4m fill above) corresponding with a load of 2350KN. From this plane, the pile-soil relative displacements become uniform and settlements are governing by the soil. Prior to it occurrence is govern by the compression in the pile element. For analysis of the strain distribution below the plane, 3000KN, assumed total depth of 85m clay, equivalent footing at neutral plane and load surface of 20x30 immediately after the fill was used.

From Figure 5.2, the average strain below the neutral plane is 1.2% and hence total settlement of 0.638m estimated below the plane.

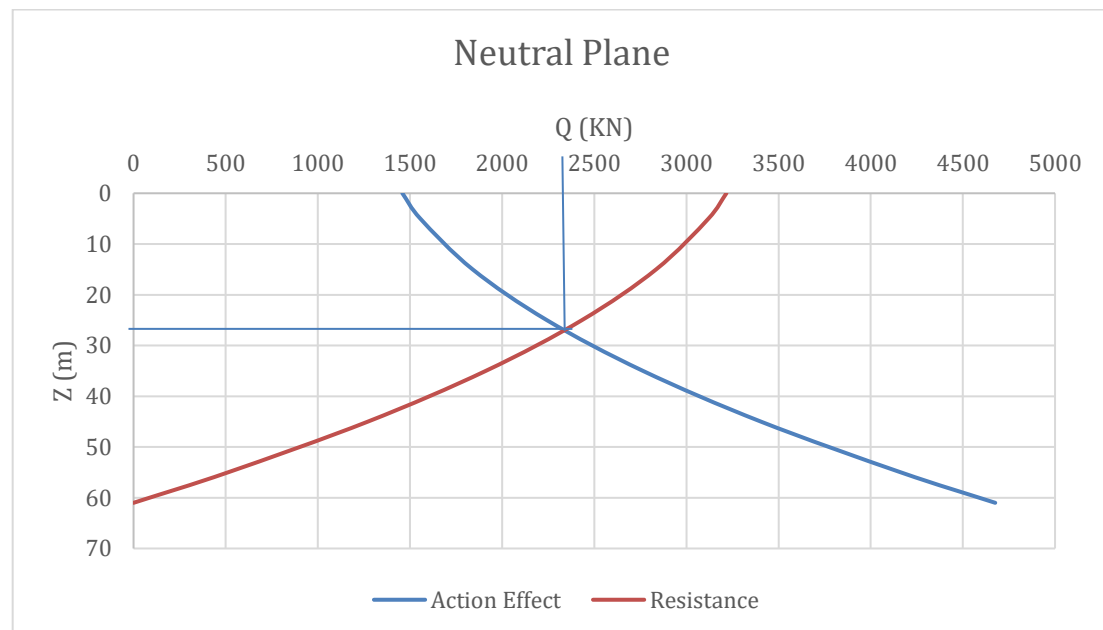


Figure 5.1: Neutral Plane

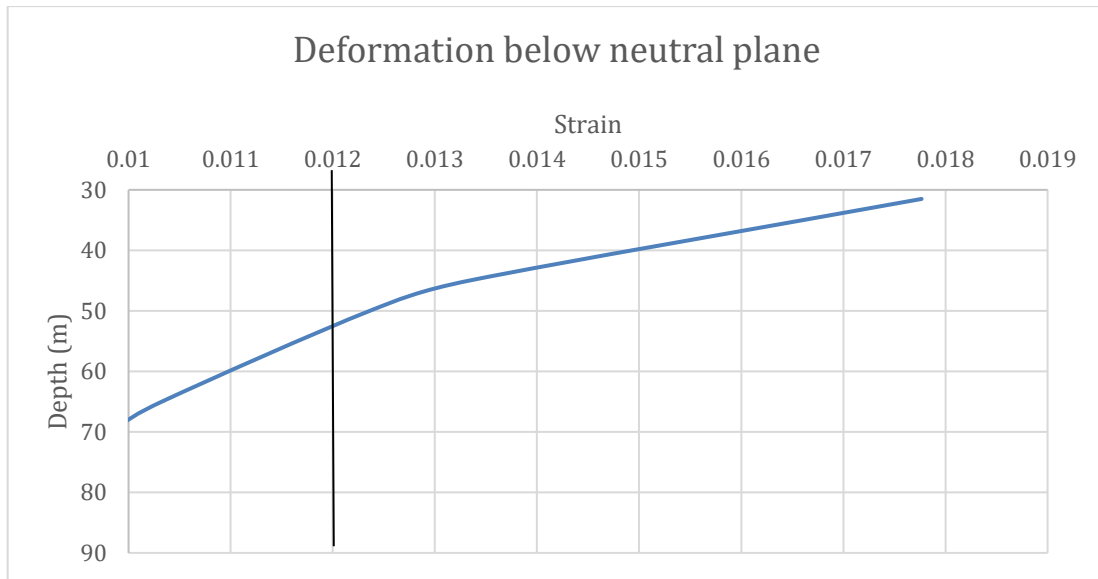


Figure 5.2: Strain in the pile below the neutral plane.

5.2 Load transfer method

The result of load transfer approach with three scenarios considered are presented and discussed in the following Sections below. For the input data and calculation sheet see appendix B2.

5.2.1 Scenario 1: Behaviour of pile as function varying pile head load

The result of load distribution and pile head displacement with varying constant pile head loads are as shown in Figure 5.3 and 5.4 respectively. As discussed previously, loads of 2000KN, 3000KN and 3500KN were used in the analysis, to study distribution behaviour along the pile shaft and its capacity. At application of 2000KN load in the analysis, at about 53m depth, mobilised base load P_b , becomes zero. Thereafter, P_b , average axial load P , and compression in pile element turned to negative values, with settlement in the pile head of 0.0268m, Figure 5.4. Indicating positive skin friction exists below depth of 53m, and toe resistance is high. This implies that about 13m length of the pile was not fully in use.

With 3000KN load, mobilised base load, compression and pile head settlement are 127.80KN, 4.4×10^4 m and 0.052m respectively. In theory, larger part of load imposed on a floating pile is distributed along the shaft. Indicating 65m length of pile is slightly low to distribute the load of 3000KN. Which results to high compression in pile element and settlement at pile head with probability of further settlement in soft clay. The behaviour of the pile with 3500KN load is similar to the 3000KN with slight increase in mobilised base load, compression and settlement at pile head as follows 411.19KN, 2.1×10^3 m and 0.068m respectively. The load distribution and load-displacement curves behaviour of pile follows the theory.

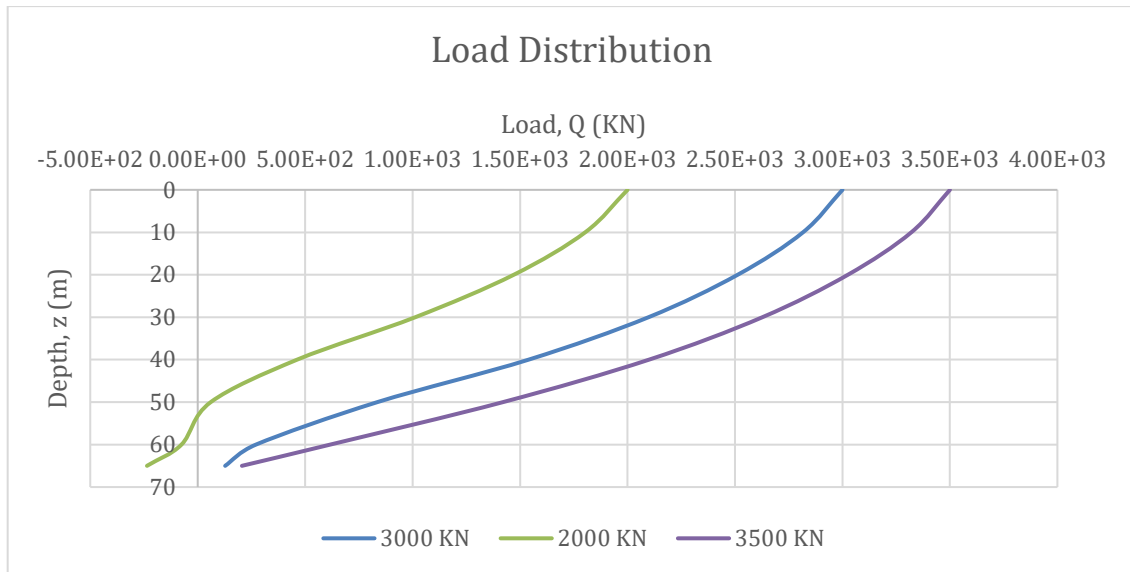


Figure 5.3: Load distribution with varying pile head load

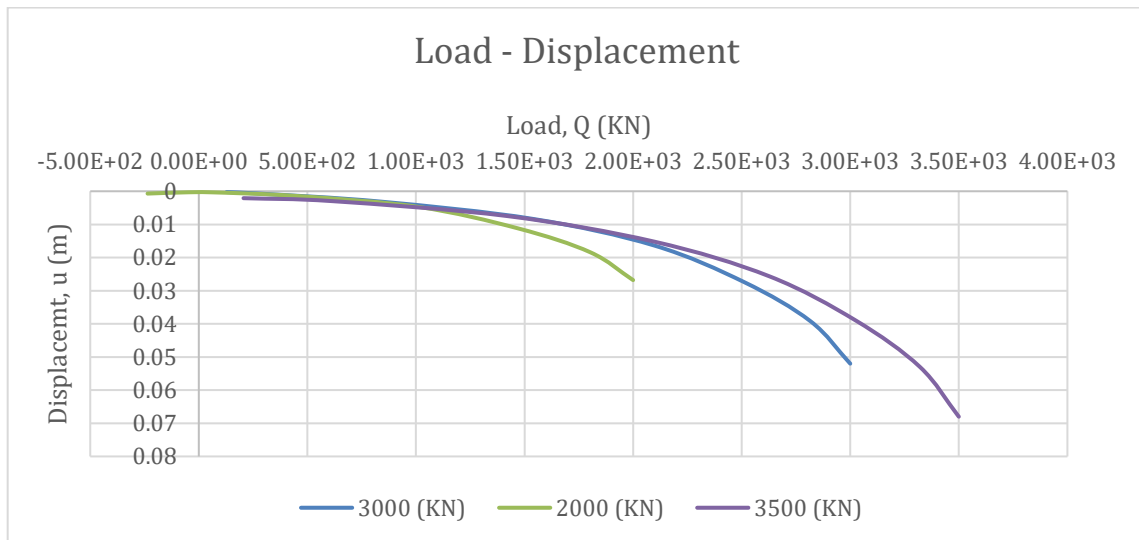


Figure 5.4: Load-displacement with varying pile head load

5.2.2 Scenario 2: Pile stiffness (modulus of elasticity) effect

In this scenario modulus of elasticity of 30GPa E , and 45GPa, E' , where compared to study behaviour of pile due to changes in its stiffness with time cause by temperature changes (heating and cooling), swelling of concrete, and reconsolidation by the soil (Fellenius B. , 2012) . With each of the modulus, the strains along the pile element where deduce with 3000KN load and plotted against depth Figure 5.7, to show likely pile deformation on site.

From Figure 5.5, at beginning part of pile element, there were no different in load bored by the pile shaft up to depth of about 43m. Between the 43 to 60m depth, the pile at elastic modulus of 45GPa shows an increase in strength and shaft absorbed more load compare to 30GPa elastic modulus. With elastic modulus of 45Gpa, the load distribution shows that the pile has more strength to withstand load.

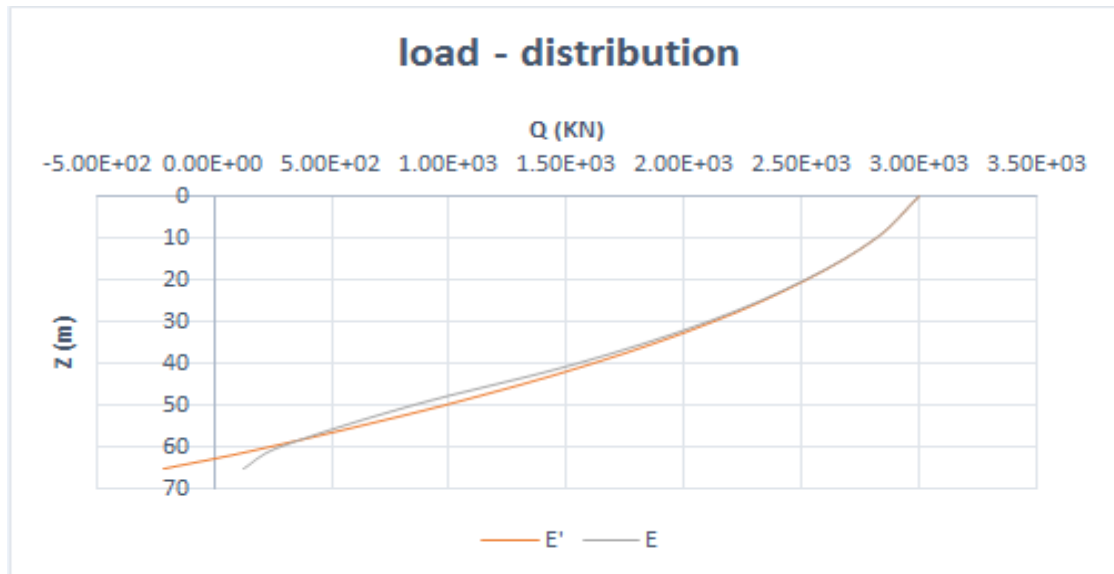


Figure 5.5: Load-distribution with different elastic modulus

Figure 5.6, shows difference in pile end displacement. At 30GPa E, mobilised base load P_b , and compression in pile SC 'at last segment are 127.79 KN and 0.00044m respectively while with 45GPa E', P_b and Sc' are -212.658KN and $4.90 \times 10^{-6}m$ respectively. This result indicate at elastic modulus of 45GPa i.e. higher concrete strength, with load of 3000KN, the pile shaft still has capacity to absorb more loads with excessive deformation in pile length.

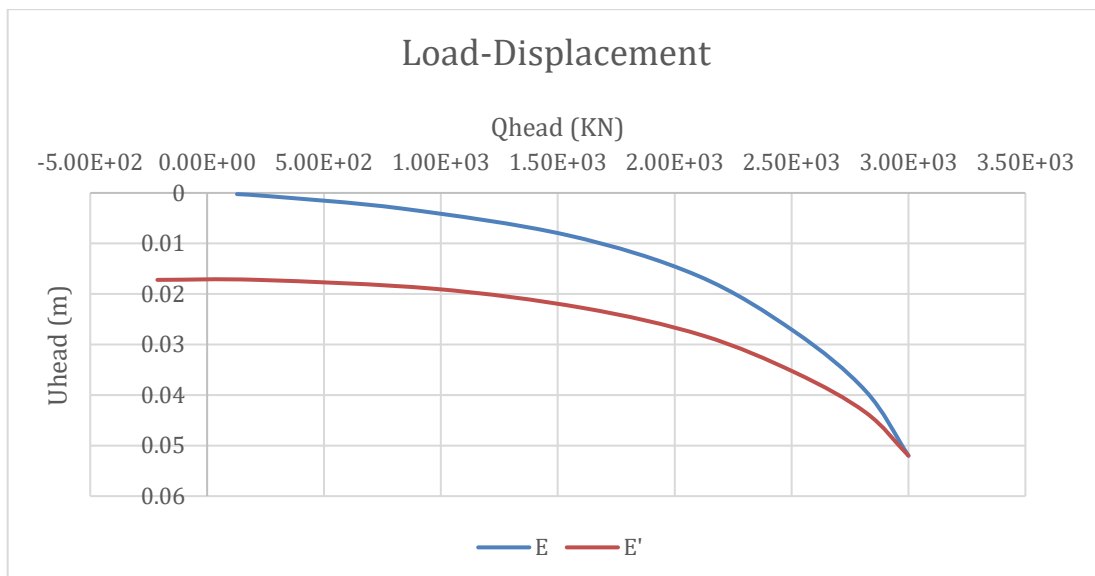


Figure 5.6: Load-displacement with different elastic modulus

Figure 5.7, illustrates Strain distributions in pile as deduced with different elastic modulus of 30GPa, E and 45GPa, E' and load of 3000KN. The Figure 5.7, shows that in both cases the strain in pile decreases with depth. With 30GPa at pile head, the strain is 1.0×10^{-4} , and 4.25×10^{-6} at 65m depth. While on 45GPa at pile head, is 6.67×10^{-5} and -4.73×10^{-6} at 65m depth. The strain distribution in the case of 45GPa, varies slightly along the pile length than in 30GPa. These indicates that the pile at elastic modulus of 45GPa has the capacity of absorbing more load and agrees with the theory, the more strength the less the deformation.

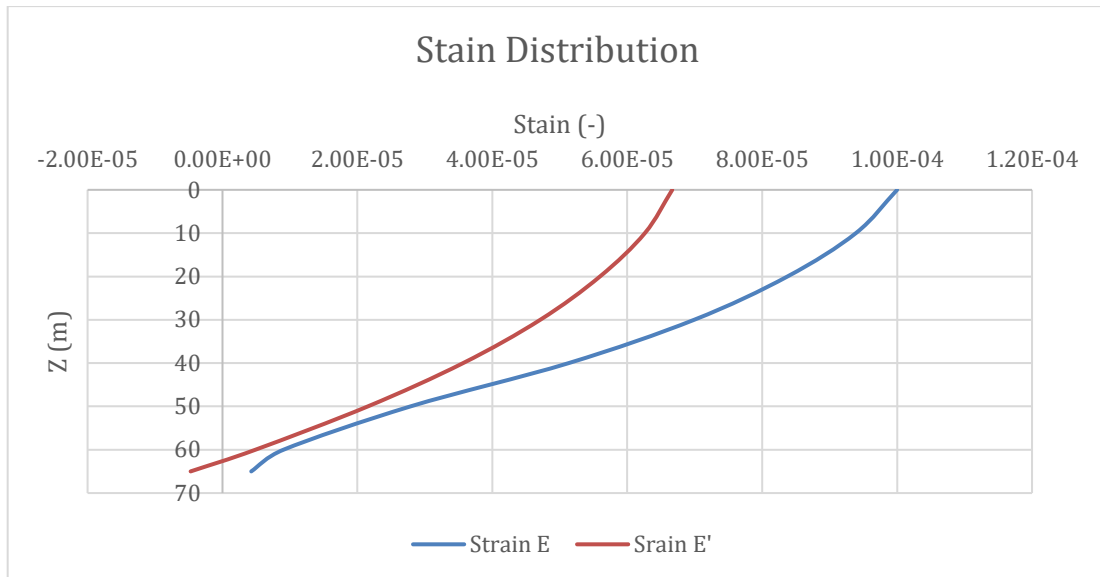
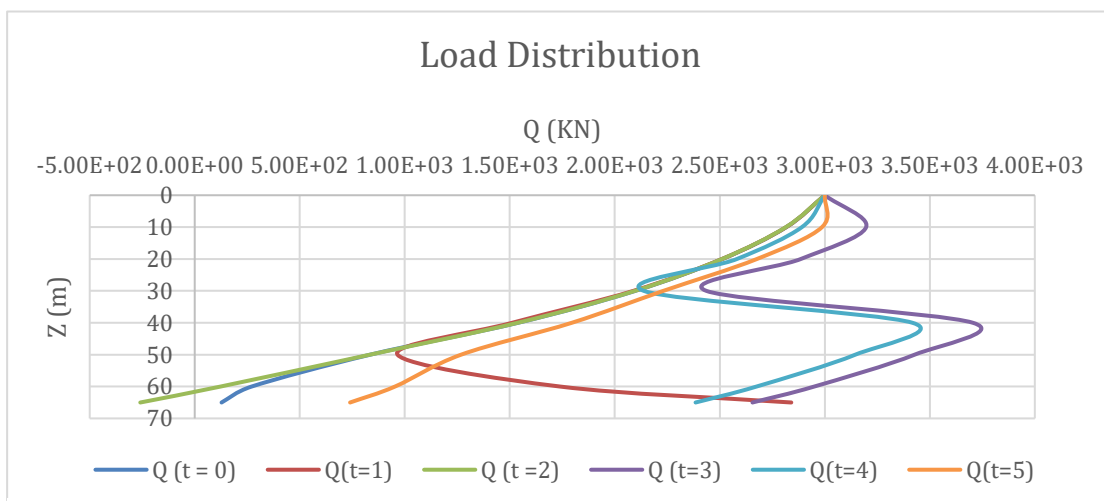


Figure 5.7: Stain distribution along the pile at different elastic modulus.

5.2.3 Scenario 3: Down drag effect

Figure 5.8 shows load distribution behaviour of pile due to superimposed settlements of soils (down drag) around the pile shaft. The Figure illustrate down drag effect at different time period, starting from the installation (no settlement) time $t = 0$ to 5 year (time $t = 0 - 5$ year) with assumed pile head load of 3000KN. The behaviour of the pile at different time agrees with Fellenius, B.H., 1984 founding, that “a static load to the pile head caused the dragload in the pile to be reduce by the magnitude of the load applied, if the applied load becomes permanent, the negative skin friction built up again and the end effect, the applied load and dragload combines in the pile.”

From Figure 5.8, curve $t = 1$, returns at certain point in load distribution to equalised the pile head load. And at $t = 2$ the negative skin friction built up again and combine with the applied pile head load to increase the magnitude of load on the pile. However, the curve $t = 2$, gives a negative mobilised base load, indicating that magnitude of negative skin friction built up is greater than the combine loads. The time, $t = 3$ and 4 also tends to equalise the load and time, $t = 5$ combines the pile head load and download to be the load acting on the pile as distributed.



6 Conclusion and Recommendation

6.1 Conclusion

The aim thesis was to study forces and displacements in long floating pile and effect of installations process on instrumentation with E45 tunnel foundation and report of previous pile instrumentation within Gothenburg as case studies. The pile analysis was performed with a single pile of 65m pile length with assumption that it will be similar with other piles.

Two different analytical methods were used, neutral plane approach and Zhang's load transfer method. The load transfer method were made in three different scenarios; function of pile head load, stiffness of pile element and down drag effects on the pile. In both methods used including scenarios employed, the results of the analysis agrees with theories of pile behaviours in soft clay. With neutral plane approach, the neutral plane was found to be at 32m depth which agrees with (Fellenius B. H., Negative skin friction and settlement of piles, 1984) that states that neutral plane is likely to occur at mid of the pile length. Total settlement below the neutral plane was 0.638m with average strain of 1.2% and capacity of pile 3582KN. With this approach, pile behaviour was good enough compared with all the theories cut across in the study.

In study of displacements and load distribution along pile shaft, with 3000KN pile head load, result of load transfer method shows that 65m length successfully distributed proposed load in agreement with known theories of floating piles. Nonlinear relationship exists between the skin resistance and displacement. Also, displacements and load distributions were linear, decreasing with depth. Pile head settlement of 0.052m, end displacement of 2×10^{-4} m with base load of 127.8kN observed.

The study of installation effects on instrumentation works, reviews that often failures occurs due to effects of vibration wave from hammer blows on the instrumented pile, calculation errors and pore water penetration into the sensitive equipment in contact with soil.

6.2 Recommendation for further study

The study of forces and displacements in long floating pile made in this thesis was based on single pile analysis in both methods employed. Grouped pile where not considered, therefore grouped pile analysis should be made to include its effect in load distribution and displacements. The piles on site where installed at depth of -12m, after excavation with intension of backfilling to the ground level. It effect to the bearing capacity of the pile where not included in the analysis in this work. Therefore, further, study should be conducted to include it.

The results from the analysis is yet to be compare with field data. Hence, field data should be collected, analysis and compare with the result to validated the analysis in this thesis.

References

- Albuquerque, P. J., Neto, O. d., & Garcia, J. R. (n.d.). Behavior Of Instrumented Omega Pile In Porous Soil. *Advanced Materials Research*.
- Bica, P., & Salgado, K. (2013). *Instrumentation and axial load testing of displacement piles*. Lyles: Lyles School of Civil Engineering Faculty Publication <http://docs.lib.purdue.edu/civeng/6>.
- Bond, A. J., & J., J. R. (2014). Effects of installing displacement piles in a high OCR clay. *Geotechnique* 41, No.3, 341 - 363.
- Claes, A. (2012). Pile Foundation - Short handbook (Educational material in Geotechnics). *version 1.1 2012*. Gothenburg: Chalmers University of Technology.
- Dembicki, G., & Horodecki, E. (2016). *Impact of deep excavation on nearby urban area*. Gdansk: Department of Geotechnics and Applied Geology, Gdansk University of technology, Poland.
- DGSI. (2017, June 20). *Slope indicator*. Retrieved from <http://www.slopeindicator.com/instruments/ext-intro.php>.
- Eslami, M., & Abolfazl, Z. (2016). Behavior of Piles under Different Installtion Effects by Physical Modeling. *International Journal of Geomechanics, ASCE*, 04016014-1 - 04016014-12.
- Fellenius, B. (2012). Discussion of "Critical assessment of pile modulus determination methods". *canadian Geotechnical Journal*, 49(5) 614-621.
- Fellenius, B. H. (1984). Negative skin friction and settlement of piles. *Second international Seminar, Pile Foundations*, (p. 12p). Singapore: Nanyang technological Institute.
- Fellenius, B. H. (2006). Results from long term measurement in piles of drag load and downdrag. *Canadian Geotechnical Journal*, 43, 409-430.
- Frank, R. (2008). Design of pile foundations following Eurocode 7-Section 7.
- Gary, A. (2000). *LONG-TERM SET-UP OF DRIVEN PILES IN SAND*. Stockholm.
- Gebreselassie, H.-G., & Berhane, K. (2006). *Excavation and Foundations in Soft Soils*.
- Hajduk, S. G., & Paikowsky, E. L. (2004). Design and Construction of Thre Instrumented Test Piles to Examine Time Dependent Pile capacity Gain. *Geotechnical Testing Journal*, 19428-2959.
- Hirsch, T. J., Coyle, H. M., Lee L. Lowery, & Charles H. Samson. (1970). Field Instrumentation for piles. *Conference on Design and Installation of pile foundations and cellular structures*. Pennsylvanianal.
- InstitutionSwedishGeotechnical. (2016). *Jords hållfasthet*,. <http://www.swedgeo.se/sv/kunskapscentrum/om-geoteknik-och-miljogeoteknik/geoteknik-och-markmiljo/jords-hallfasthet/skjuvhallfasthet/>.
- Jardine, A. J., & Richard, B. (1991). Effect of installing displacement piles in a high OCR clay.
- Jardine, B. M., & Lehane, J. R. (1994). Displacement-Pile behaviour in a soft marine clay. *Canadian Geotechnical Journal*, Vol: 31, 181-191.
- Karlsson, M., Emdal, A., & Dijkstra, J. (2016). Consequences of sample disturbance when predicting long-term settlements in soft clay. *Canadian Geotechnical Journal*, Vol:53(dx.doi.org/10.1139/cgj-2016-0129), 1965-1977.
- Kim Malcolm. (2014). Vibrating wire rebar strain gauge user manual. *Vibrating wire rebar strain gauge user manual*.

- Knappett, & Craig, J. (2012). *Craig's Soil Mechanics, Eighth Edition*. Dundee, UK: CRC Press.
- Kovacs, R. D., & Holtz, W. D. (1981). *Introduction to Geotechnical Engineering*.
- Lönnroth, L. (2000). *Option på framtiden: den värderingsstyrda ekonomin*. Stockholm.
- Medin, F., & Johanna, B. (2015). *Analysis and modelling of settlements of*. Gothenburg.
- Mohamad, H., Soga, K., & Bennett, P. (2009). Fibre optic installation techniques for pile instrumentation. *Processing of the 7th International Conference on Soil Mechanics and Geotechnical Engineering*, (pp. 1873 - 1876).
- Nguyen, H., & David, H. (2016). *Analysis and FE-modelling of Soil displacement associated to pile driving*. Gothenburg: Chalmers University of Technology.
- Ottolini, M., Dijkstra, J., & Tol, F. v. (2015). Immediate and long-term installation effects adjacent to an open-ended pile in a layered clay. *Canadian Geotechnical journal* 52, www.nrcresearchpress.com/cgj, 982-991.
- Peter Claesson, Gunnar Holmberg, & Romell, J. (2007). *Höghus Lilla Bommen, Göteborg Uppföljning av kohesionpåblning i mäktiga lerlager*. Göteborg.
- Poulos, H. (1994). Effect of pile driving on adjacent piles in clay. *Canadian Geotechnical Journal*, 31(6) 856-867, 10.1139/t94-102.
- Randolph, M., Carter, J. P., & Wroth, C. (1979). Driven piles in clay-the effects of installation and subsequent consolidation. *Geotechnique*, 29 No. 4, 361 - 393.
- Randolph, M., Carter, J. P., & Wroth, C. (1979). The effects of installation and Subsequent consolidation.
- Rao, V. R. (2009, 03 04). *Pile Foundation*. Retrieved from https://www.slideshare.net/_ram/pile-foundation.
- Ruul, P., & Johanna, N. (2011). *Environmental impact of pile driving*. Göteborg.
- Sew, G. S., & Meng, C. c. (2017, 04 17). *Piled Foundation Design and Construction*. Retrieved from <http://www.gnpgeo.com.my>.
- Terzaghi, K. (1943). *Theoretical Soil Mechanics*. John Wiley & Sons, Inc.
- The constructor, c. E. (2017, 06 07). *Pile installation methods*. Retrieved from <https://theconstructor.org/geotechnical/pile-installation-methods/1812>.
- Tho, k. k., Chen, Z., Leung, C. F., & Khoo, C. Y. (2014). Enhanced analysis of pile flexural behavior due to installation of adjacent pile. *Canadian Geotechnical Journal* 51(6):, 705 - 711, 10.1139/cgj-2013-0215.
- Wersall, K., & Carll, R. M. (2013). Cumulative Soil Displacement due to pile Driving in Soft Clay. *Sound Geotechnical Research to Practice, Geotechnical Special Publication (GSP 230)*, ASCE, 463 - 480.
- Yanne, J. (2016). *On the long-term behaviour of tension loaded piles in natural soft soils : A field study and numerical modelling*. Göteborg: Chalmers University of Technology.
- Zhang, Q.-q., & Zhang, Z.-M. (2012). A Simplified nonlinear approach for single pile settlement analysis. *Canadian Geotechnical Journal* 49.11, 1256-1266.

